Polymer Degradation and Stability 250 (2026) 112148

Contents lists available at ScienceDirect

Polymer Degradation and Stability

journal homepage: www.journals.elsevier.com/polymer-degradation-and-stability

Harnessing microbial consortia-based bioprocess for polyolefins waste upcycling to polyhydroxyalkanoates: optimization of a fed-batch process with hybrid feeding strategy

Passanun Lomwongsopon [a], Tanja Narančić [b], Reeta Davis [c], Meg Walsh [c], Kevin E. O'Connor [b,c], Cristiano Varrone [a,*]

[a] Section of Bioresources and Process Engineering, Department of Chemistry and Bioscience, Aalborg University, Fredrik Bajers Vej 7H, 9220, Aalborg, Denmark
[b] School of Biomolecular and Biomedical Science, and BiOrbic - Bioeconomy Research Centre, University College Dublin, Belfield, Dublin 4, Ireland
[c] Bioplastech Ltd., NovaUCD, Belfield Innovation Park, University College Dublin, Belfield, Dublin 4, Ireland

ARTICLE INFO

Keywords:
Bioupcycling
Polyolefin pyrolysis wax
Bioconversion
Mixed microbial consortia
Defined mixed consortia
PHA
Bioplastics
Fed-batch reactor
Advanced feeding strategy

ABSTRACT

The linear plastic value chain and the inefficient end-of-life management raise significant environmental concerns. As closed-loop recycling alone cannot effectively handle mixed post-consumer plastics, with polyolefins (PO) representing 40% of it, innovative strategies are needed to complement recycling and avoid mismanagement of plastic waste. Currently, there is no "one-fits all" solution to solve the plastic waste challenge, but a proper integration of different technologies could provide a substantial contribution. Here, we demonstrate a tandem process combining pyrolysis and microbial consortia-based biotechnological conversion to upcycle PO waste into the biodegradable polymer polyhydroxyalkanoate (PHA). Using a top-down and bottom-up eco-engineering approach, we developed efficient PO pyrolysis wax-utilizing mixed microbial consortia (MMC) and defined mixed consortia (DMC). Under nitrogen-limiting conditions in shake-flask experiment, DMC of *Serratia nematodiphila* and *Cupriavidus necator* H16 produced 193.0 ± 4.3 mg/L PHA, comparable to enriched MMC (138.6 ± 51.5 mg/L). Employing batch fermentation with pulse-feeding of PO wax increased PHA titer of the MMC process by 4.4-fold in shake-flask, while no change or even decrease in titer was observed in DMC, likely due to inhibition and altered interspecies interactions. Consequently, 1.5 L-fed-batch fermentation with hybrid feeding strategy (exponential feeding, followed by pulse feeding) was further developed to increase PHA titer, yield, and productivity from the MMC process. The final titer at 96 h was 772.1 ± 93.3 mg/L, or 5.6-fold improved from unoptimized shake-flask process. PHA yield and productivity peaked at 50 h, achieving 0.049 ± 0.005 gPHA/gPOwax-added, and 13.2 ± 1.4 mg/L/h, representing 2-fold and 1.5-fold increases, respectively, compared with the unoptimized feeding scheme. The results represent the highest reported PHA titer from non-oxidized PO pyrolysis wax, achieved solely through optimization of fed-batch feeding strategy relying solely on PO wax.

1. Introduction

Plastic production uses 8 % of global crude oil consumption and contributes to 3.3 % of global greenhouse gas emission [1,2]. Given the current poor recycling rate of <10 %, the plastic value chain is still mostly linear, causing environmental pollution and inefficient use of fossil feedstock, as it is locked in the non-renewable recalcitrant plastics [3,4]. The consumer behavior and single-use culture of plastic commodity materials have surpassed the projections of global plastic accumulation rate. As the world's plastic production and consumption are projected to triple by 2060, a different circularity thinking in the plastic value chain needs to be implemented to reduce the negative impact of post-consumer plastics [5]. A European Strategy for Plastics in a Circular Economy was launched by the European Commission in 2018, stating that all plastic packaging placed on the EU market is expected to be either reusable or recyclable in a cost-effective manner by 2030. Given the current state of recycling, novel and complementary technologies are very much needed to achieve such goal.

* Corresponding author.
E-mail address: cva@bio.aau.dk (C. Varrone).

https://doi.org/10.1016/j.polymdegradstab.2026.112148
Received 9 March 2026; Received in revised form 12 April 2026; Accepted 20 April 2026
Available online 22 April 2026

Biotechnology approach can give added value to plastic waste (so-called "bio-upcycling"). Using plastic waste as a biorefinery feedstock in addition to conventional biomass to produce renewable plastics promotes circularity in the plastic economy and could even lead to enhanced polymer functionalities [6,7]. To give examples of such process, ethylene glycol and terephthalic acid from enzymatically hydrolyzed polyethylene terephthalate (PET) can be upcycled to poly (ethylene furanoate) (PEF), polyhydroxyalkanoates (PHA), and poly (amide urethane) via microbial conversion processes [6–9]. Even though such processes would be ideal for post-consumer plastic upcycling, most studies focus on PET, which represents only 6 % of global plastic waste, because the enzymatic hydrolysis process for PET depolymerization has already been demonstrated and is currently being scaled-up by Carbios. Unlike PET, recalcitrant polyolefins (PO) are unhydrolyzable due to their C-C backbone and high crystallinity, and the discovery of efficient depolymerization enzymes on real PO waste is still a major challenge [10,11]. However, PO are heavily used for short shelf-life packaging material, representing >45 % of world plastic production in 2024; thus, this fraction cannot be ignored [3,12]. Due to the extreme recalcitrance of PO toward biological depolymerization, an integrated process, in which PO are first depolymerized by thermochemical processes (e.g., pyrolysis, hydrogenolysis, liquefaction, etc.) [13–16], and then valorized through the bio-upcycling of the lower value deconstructed products (such as pyrolysis waxes), represents a more promising approach.

PHA belong to a family of microbial polyesters and can be used as bio-based biodegradable thermoplastic [17]. PHA are accumulated intracellularly under environmental imbalanced conditions such as nutrient (nitrogen, phosphorus, and sulfur) limitation, excessive carbon, and alternate oxygen deficiency [18]. PHA have a wide diversity of monomers, resulting in variations in polymers and copolymers, leading to different properties. Thus, they can replace some fossil-based plastics in a range of applications, e.g., consumer goods, packaging, medical appliances, and agricultural films [19]. According to the Waste Framework Directive, bio-based and biodegradable/compostable plastics hold great potential for food-contaminated packaging or in cases where waste collection is impossible [20]. Upcycling conventional plastic waste into biodegradable plastics like PHA addresses all aspects of plastic waste management by giving value to end-of-life materials and producing new materials with lower environmental hazards.

Microbial mixed cultures have been applied in different bioprocesses, including PHA production, and shown to be more advantageous than monocultures in many aspects [21]. Mixed cultures can provide complementary metabolic pathways to catabolize a wide range of complex/recalcitrant substrates and channel them for PHA production under favorable conditions, overcoming the limitation of the metabolic capacity of a single strain and its low conversion efficiency [22,23]. Open mixed microbial consortia (MMC) have the advantage of operating under non-sterile conditions and provide versatility in using contaminated substrates [17]. For example, an enriched MMC dominated by *Xanthobacter, Rhodococcus, Paracoccus,* and *Acinetobacter* was shown to accumulate PHA (0.42 CmolPHA/CmolSubstrate) from crude glycerol fermentation effluent (composed of volatile fatty acids (VFA) and 1,3-propanediol) [24]. PHA production (0.31–0.32 CmolPHA/CmolSubstrate) was also obtained from bio-oil, a complex mixture of alcohols, aldehydes, ketones, carboxylic acids, and other polar components, by MMC [25]. Use of artificial microbial consortia, or defined mixed consortia (DMC), in which a number of known microbes are co-cultured, is another mixed culture strategy that can lead to improved performance in specific applications, depending on the design of the consortium [26]. DMC constructed with synergistic substrate degraders and PHA producers were shown to accumulate high levels of PHA. For instance, the DMC composed of inulinase enzyme producer *Bacillus gibsonii* and PHA producer *Cupriavidus necator* was able to accumulate up to 80 % of PHA in cell biomass from inulin (a polysaccharide found in the roots and tubers of various crops) [27].

To date, there has been very limited research exploring mixed culture processes for PHA production from conventional plastic waste. This study aims to select and design microbial consortia capable of producing PHA solely from PO pyrolysis wax by employing two engineering strategies: a top-down approach (for MMC) and a bottom-up approach (for DMC). These processes are expected to harness the robustness and resilience of microbial consortia, enabling the direct upcycling of PO pyrolysis wax without additional chemical pretreatment typically used to pre-oxidize the wax [16,28], facilitating its bioavailability for microbial uptake. Additionally, bioprocess optimization through refining the feeding strategy for fed-batch fermentation was performed to improve PHA titer, yield, and productivity, promoting scalability and preparing the transition from laboratory towards larger-scale processes.

2. Materials and methods

2.1. Enrichment and assembly of microbial consortia

Top-down engineering of MMC: The soil and leachate samples were collected from a plastic landfill located in Avedøre (Greater Copenhagen Area) and enriched on Mineral Salt media (MSM) [29] with 10 g/L PO wax at 30 °C and 150 rpm. The enrichment was performed by subculturing every four weeks during the first three cycles and then every two weeks for the rest five cycles to select PO wax-degrading MMC. In our previous study, adaptive laboratory evolution (ALE) was then performed by transferring logarithmic growth MMC to fresh medium for several cycles, with stepwise increased PO wax concentration from 10 to 60 g/L from various substrates. 16 s full-length amplicon sequencing (PacBio Sequel II/IIe) was used to analyze microbial diversity in enriched and adapted MMC [30]. The best performing MMC, namely W2-ALE, was used in this study. It is comprised of *Stenotrophomonas* (57.4 %), *Sphingobacterium* (17.3 %), *Ochrobactrum* (6.1 %), and *Achromobacter* (4.8 %) as the dominant genera. Other known PHA producing genera, such as *Pseudomonas* (1.3 %) and *Xanthobacter* (1.5 %) were also present in the consortium.

Bottom-up engineering of DMC: Enriched MMCs (after 7th subculturing cycle) were used as the source for bacterial isolation by the traditional spread plate technique on MSM agar plates containing 1 g/L PO wax and supplemented with 0.02 g/L yeast extract. Single colonies were transferred to LB agar plates and re-streaked several times to obtain single isolates. Cryostocks were prepared in LB media with 30 % glycerol and stored at -80 °C. 15 distinct colonies were isolated, and Sanger sequencing of 16 s rRNA (Eurofins Genomics, Cologne, Germany) was performed to identify bacterial species. The isolates, excluding the (potential) pathogenic bacteria, were individually tested for their ability to utilize PO wax (10 g/L), and those with high growth were selected for DMC screening experiments (Fig. S1).

Three isolates, identified as *Acinetobacter proteolyticus* NIPH 809 (Ap), *Pseudomonas plecoglossicida* NBRC 103162 (Pp), and *Serratia nematodiphila* DSM 21430 (Sn) (99.51 %, 99.49 %, and 99.51 % similarities, respectively), were subjected to whole genome sequencing by llumina NovaSeq 6000 platform (GENEWIZ, Azenta Life Sciences, Leipzig, Germany) and used in this study as PO wax degraders. Known PHA-producing bacteria, including *Cuprividus necator* H16, *Pseudomonas putida* KT2440, *Pseudomonas umsongensis* GO16, and *P. umsongensis* GO16 *ΔlysR*, were combined with the PO wax degraders to construct 2–3 membered DMCs. All DMCs were prepared by mixing the 18-h-old monocultures of each strain (adjusted to an OD600 of 1.0) at the ratio of 1:1 (or 1:1:1). The final OD600 of constructed DMCs was 1.0, and 10 % (v/v) of these DMCs were used for inoculation in shake-flask PHA production experiment. PHA production from the DMCs was compared to that of individual monocultures and the MMC.

2.2. PHA production media and shake-flask PHA production experiment

PHA production media contained 2.2 or 10 g/L PO wax emulsion

(1.86 or 8.62 gC/L) (if not stated otherwise), nitrogen source at 0.065 gN/L (nitrogen-limiting condition) or 0.26 gN/L (nitrogen-non-limiting condition) (if not stated otherwise), 9 g/L $Na_2HPO_4 \bullet 12H_2O$, 1.5 g/L KH_2PO_4, 200 μg/mL $MgSO_4 \bullet 7H_2O$, 2 mg/L $ZnSO_4 \bullet 7H_2O$, 1 mg/L $CaCl_2 \bullet 2H_2O$, 5 mg/L $FeSO_4 \bullet 7H_2O$, 0.17 Na_2MoO_4, 0.2 mg/L $CuSO_4 \bullet 5H_2O$, 0.4 mg/L $CoCl_2 \bullet 6H_2O$, 1.22 mg/L $MnCl_2 \bullet 4H_2O$, and 10 mg/L EDTA. PO wax-in-water emulsion was prepared by mixing the desired amount of melted PO wax with an oil-soluble surfactant, Span 80 (0.1 % w/v), at approximately 80 °C, while in another beaker, mixing sterile distilled water with a water-soluble surfactant, Tween 20 (0.1 % w/v), at approximately 85 °C. The wax phase was dropwise added into the water phase under stirring to create emulsion, followed by ultrasonication for 10 min (30 s on and 30 s off interval at 80 % amplitude). PO wax from commercial pyrolysis of mixed PO was provided by Waste Plastic Upcycling (WPU) Denmark (Vitol), containing 91.6 % alkanes, 7.8 % alkenes, and 0.6 % aromatics [30]. Aliphatic hydrocarbon composition in this PO wax ranged from C12 to C40, as demonstrated by the gas chromatography–mass spectrometry (GC–MS) chromatogram (Fig. 1). Carbon and nitrogen were shown to be 86.21 % and 0.35 % by weight of PO wax, analyzed by an elemental analyzer (Flash*Smart*™, Thermo Scientific).

The shake-flask batch PHA production experiments were carried out in 250 mL-flasks with the working volume of 50 mL at 30 °C and 200 rpm for 48 h. For shake-flask batch with pulse-feed, batch cultivation with a starting volume of 50 mL was performed for 24 h, then a small volume of concentrated PO wax emulsion (20 g/L) in MSM without nitrogen addition was pulse-fed twice every 16 h interval to achieve a final PO wax concentration of 2 g/L per pulse in the flask. Prior to each pulse-feeding, 5 mL of culture was withdrawn for further analysis. The inocula for each experiment were harvested from 18-h-old MMC or DMC at the OD600 of 1.0 with the inoculum size of 10 % (v/v); the starting OD600 in flasks was 0.1. Cells were collected and freeze-dried for cell dry weight (CDW) and PHA content analysis.

2.3. Bioreactor-scale PHA production by fed-batch with hybrid feeding strategy

Bioreactor-scale PHA production was carried out in 1.5 L-Twin Modular Bioreactors (KBiotech, Switzerland). Fed-batch cultivation was performed, starting with 24 h-batch operation under nitrogen-non-limiting condition, followed by fed-batch for the rest of cultivation time until 96 h. The pH (EasyFerm Bio HB Arc, Hamilton, Switzerland), DO (VisiFerm DO Arc H0, Hamilton, Switzerland), and temperature (PT100 Evomini#M-3, Italcoppie, Italy) probes were connected to the bioreactor's vessels to monitor cultivation conditions. The pH was maintained at 7.0 with the addition of 1 M NaOH or 1 M H_2SO_4. Dissolved oxygen (DO) was controlled at 20 % by cascade control of agitation rate (150–750 rpm) and aeration rate (compressed air at 0–1 NL/min). The temperature was controlled by a water jacket at 30 °C.

The fermentation started with an initial batch phase with a working volume of 278 mL of 1.1 g/L PO wax emulsion in MSM and 1.58 g/L $NaNO_3$ (10 % (v/v) inoculum at OD600 = 1.0, resulting in an initial OD600 of 0.1 in bioreactor). For the following fed-batch phase, feeding strategy (including exponential feeding and pulse feeding) was optimized to achieve higher cell biomass and PHA production. As PO wax is not soluble in water, the feed tanks were prepared by emulsifying relatively low concentrations of 10 and 20 g/L PO wax in MSM, with 1.58 g/L $NaNO_3$ and without $NaNO_3$, for exponential and pulse feeding, respectively. Substrate concentration required to produce biomass Xt at time t during exponential feeding was calculated based on the following equation:

$$S_t = \left(X_0 \,/\, Y_{x/s}\right) e^{\mu t} \tag{1}$$

where X_0 is the initial biomass (gCDW/L), $Y_{x/s}$ is biomass yield identified from preliminary batch cultivation, and μ is fixed at 75 % of average specific growth rate identified also from preliminary batch cultivation.

Samples were taken periodically for the analysis of OD600, CDW, PHA content, and PO wax concentration.

2.4. Substrate, nitrogen, and PHA content analysis

Substrate (PO wax) quantification was analyzed by GC–MS analysis of hydrocarbon concentrations in the dichloromethane (DCM) extracted samples. Samples and DCM were mixed in the ratio of 1:1 by vigorously shaking for 30 min. Then, the samples were settled to allow phase separation, and the DCM phase was transferred to the GC vials for subsequent analysis by a GC (Agilent Intuvo 9000) equipped with an Agilent DB-5 ms column (30 m × 250 μm × 0.25 μm) and a high-resolution MS (Agilent 7010B Triple Quadrupole) with liquid injection field desorption ionization, using the following program: injection temperature of 350 °C, column temperature program of 35 °C (2 min), using a ramp at the rate of 25 °C/min to 100 °C, then at the rate of 50 °C/min to 350 °C and hold at 350 °C (6.5 min).

The samples were centrifuged at 8000 rpm for 10 min, and the supernatants were filtered through 0.45 μm pore sized syringe filters for nitrogen quantification assay. Nitrate TNTplus Vial Test (TNT835, HACH Lange, Denmark) was used to quantify nitrogen concentration, in the form of NO_3-N (mg/L).

Cell pellets after removing supernatants were washed with 0.1 M

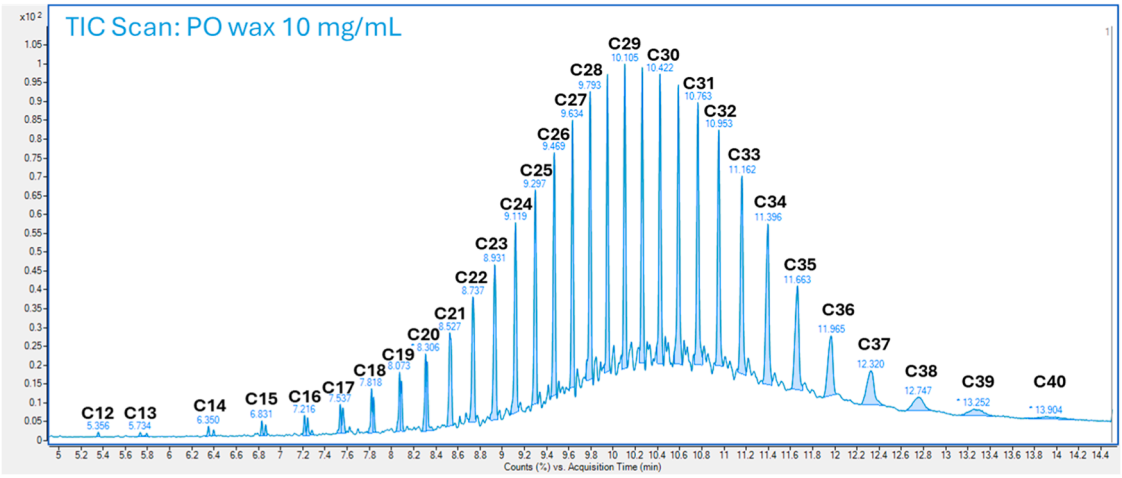

Fig. 1. Total ion chromatogram of PO wax (10 mg/mL in dichloromethane). Aliphatic hydrocarbons ranging from C12 to C40 were detected, accounting for up to 99.4 % by weight of PO wax.

phosphate buffer and subjected to freeze-drying. Freeze-dried biomass (5–10 mg) was used for PHA content (%PHA per CDW) and PHA monomer composition analysis using acidic methanolysis method, described in our pervious publication [30]. 3-Hydroxyalkanoic acid methyl esters, the products from acidic methanolysis reaction, were subjected for GC analysis (TRACE™ 1310, Thermo Scientific), equipped with a ZB-FAME column (30 m x 250 μm x 0.20 μm) and a flame-ionization detector (FID). Helium was used as a carrier gas at the constant flow rate of 1.0 mL/min. The injection temperature was 270 °C (split ratio of 50:1). The heating program was as follows: 120 °C for 5 min, ramped to 180 °C at the rate of 10 °C/min and held for 1 min, then ramped to 250 °C at the rate of 10 °C/min and held for 5 min. The methyl esters of PHA monomers ((*R*)-3-hydroxyalkanoic acid) from C4–12 were used as standards to identify retention times.

3. Results and discussions

3.1. Isolation of PO wax degrading strains and whole genome sequencing

Bacteria were isolated from PO wax-enriched microbial consortia by spread plate technique. Distinct colonies were identified via 16s rRNA amplicon sequencing. The isolates were then cultivated in a modified MSM medium using emulsified PO wax/mineral oil blend (1:1 w/w) as a carbon source. *Acinetobacter proteolyticus* (Ap), *Pseudomonas plecoglossicida* (Pp), and *Serratia nematodiphila* (Sn) exhibit the best growth on PO wax as a monoculture and were subjected to whole-genome sequencing by the Illumina NovaSeq platform (Fig. 2).

Draft genomes of Ap, Pp, and Sn exhibited high completeness (100 %, 99.92 %, and 99.85 %, respectively), with low contamination of foreign DNA sequences (1.74 %, 0.99 %, and 0.89 %). The genome characteristics of Ap, Pp, and Sn are given in Table 1. Overall, 2594, 5543, and 5031 genes were predicted in Ap, Pp, and Sn, respectively. Several annotated genes were likely associated with enzymatic functions involved in petroleum or hydrocarbon degradation. For example, alkane monooxygenases, which are alkane-degrading enzymes distributed among many different microorganisms [31], cytochrome P450s, which are the monooxygenases catalyzing the oxidation of aliphatic hydrocarbons (C5-C16) [32], catechol dioxygenases, a class of bacterial iron-containing enzymes involved in aerobic aromatic hydrocarbon degradation [31], were present in all three isolates. Additionally, several enzymes involved in hydrocarbon degradation pathways, for instance, alcohol dehydrogenases, aldehyde dehydrogenases, esterases, and laccases, were also found across the three isolates, indicating available hydrocarbon degradation machineries that could be relevant to PO wax biodegradation.

Table 1
Genome annotation and features.

Characteristics	*A. proteolyticus*	*P. plecoglossicida*	*S. nematodiphila*
GC content (%)	41.6	62.4	59.3
No. of coding sequences	4535	5900	5781
No. of characterized proteins	2718	4124	4200
No. of hypothetical proteins	1817	1776	1581
No. of RNAs	69	64	79
Size (bp)	4,490,196	6,083,677	5,513,496

In addition, genes related to PHA metabolism, such as PHA synthase, PHA granule-associated proteins PhaF and PhaI, and PHA depolymerase, were also present in Ap and Pp (but not Sn), suggesting the potential of the two isolates as PHA-producing strains.

3.2. Construction of DMCs for PHA production test in comparison with MMC in flask-scale

Isolated PO wax degraders (Ap, Sn, and Pp) and known PHA producers (*C. necator* H16, *P. putida* KT2440, *P. umsongensis* GO16, and *P. umsongensis* GO16 *ΔlysR*) were tested individually and as a co-culture

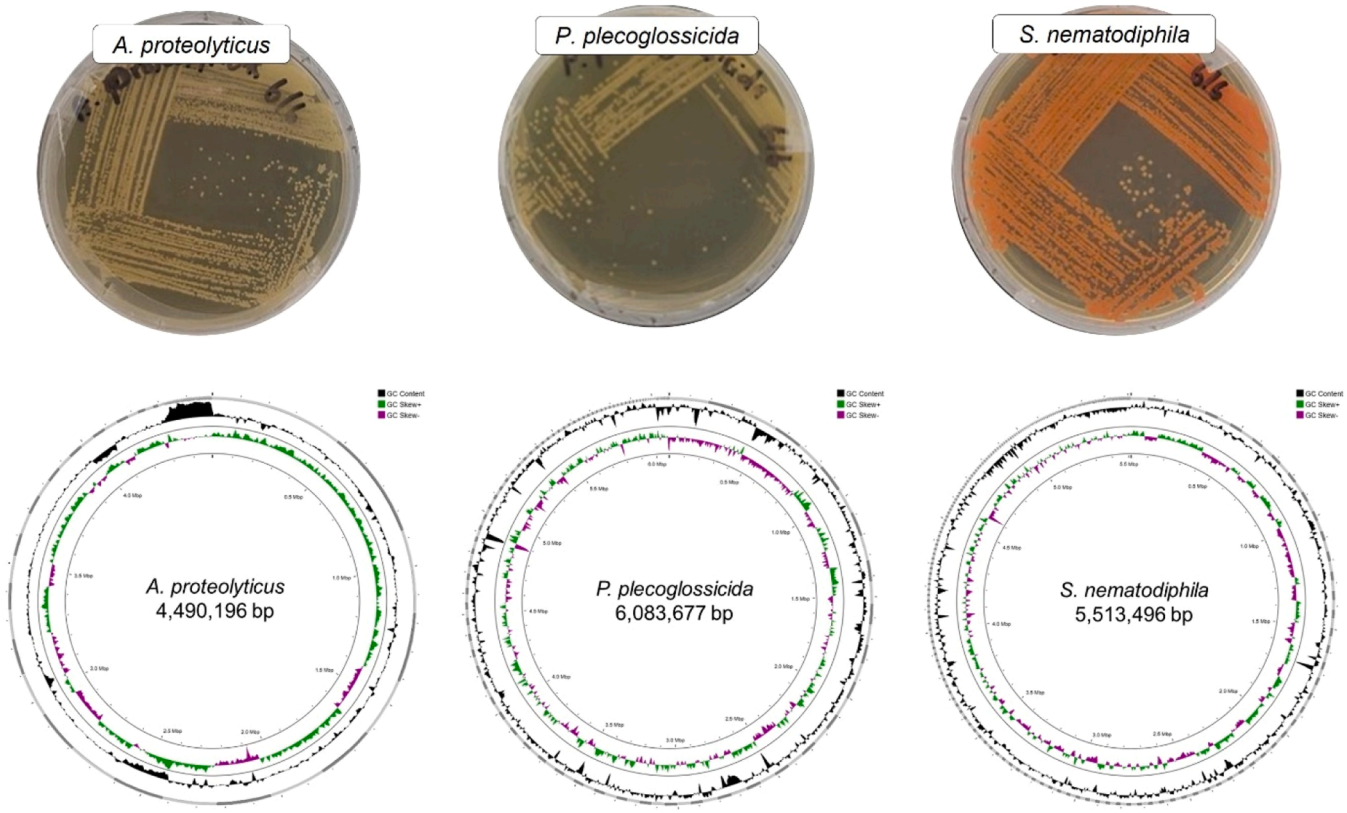

Fig. 2. Three PO wax-degrading isolates and their graphical map of complete genomes.

for PHA production in MSM using 2.2 g/L (1.86 gC/L) PO wax as a carbon source at nitrogen-non-limiting (0.26 gN/L) or limiting (0.065 gN/L) condition. Two-membered DMCs were constructed by pairing one PO wax degrader with one known PHA producer. In addition, three-membered DMC consisting of Ap, Sn, and Pp was also tested as Ap and Pp showed the ability to accumulate PHA from both PHA-unrelated (glucose) and related (octanoate) substrates during the preliminary test (Table S1). The adapted MMC (subsequently referred to as W2-ALE) was tested in parallel to compare the PHA production with the DMCs.

As expected, the nitrogen-non-limiting condition (shown in Fig. 3a) supported better growth and resulted in higher cell biomass concentration, especially for Ap and the DMCs with Ap as a member. The average cell biomass concentration was 1.90 ± 0.07 gCDW/L, which is approximately 3 times higher than the amount produced under nitrogen-limiting condition (0.66 ± 0.05 gCDW/L). As a monoculture, all *Pseudomonas* strains (Pp, KT2440, GO16, and *ΔlysR*) were able to grow on PO wax, but low biomass was observed in both nitrogen-non-limiting (0.18–0.29 gCDW/L) and limiting condition (0.21–0.33 gCDW/L). Ap, Sn, and H16 produced more than two-fold higher biomass than *Pseudomonas* strains (both under nitrogen-non-limiting condition: 1.80 ± 0.01, 0.43 ± 0.04, and 0.83 ± 0.01 gCDW/L, respectively, and nitrogen-limiting condition: 0.60 ± 0.01, 0.67 ± 0.07, 0.64 ± 0.01 gCDW/L, respectively). For co-cultures, positive interaction was found only in the DMC of Pp+KT2440 when using nitrogen-non-limiting condition, as can be seen from increased biomass production from 0.28 ± 0.02 (Pp) and 0.18 ± 0.02 (KT2440) gCDW/L to 0.91 ± 0.04 gCDW/L (Fig. 3a). However, PHA accumulation under nitrogen-non-limiting condition was generally low for every monoculture, DMC, and MMC (average of 1.4 ± 0.8 % per CDW), except for GO16 (7.7 ± 0.3 % per CDW), *ΔlysR* (21.4 ± 1.2 % per CDW), and their DMCs with Sn (Sn+GO16: 10.1 ± 3.3, Sn+*ΔlysR*: 18.7 ± 0.4 % per CDW) (Fig. 3b). The nitrogen-limiting condition led to higher PHA accumulation, as expected (Fig. 3c). Interestingly, even if the DMCs with Sn as a member did not show much higher biomass production than monocultures, they reached significantly higher PHA accumulation. Sn+H16, Sn+KT2440, Sn+GO16, Sn+ *ΔlysR*, and Sn+Pp accumulated PHA at 24.4 %, 7.3 %, 11.5 %, 13.0 %, and 5.2 % per CDW, respectively, whereas H16, KT2440, GO16, *ΔlysR*, and Pp monoculture accumulated 15.8 %, 1.6 %, 6.9 %, 14.0 %, and 1.0 % per CDW, respectively. Sn by itself showed no PHA production. Maximum PHA titer of 193.0 ± 4.3 mg/L was achieved by using the co-culture of Sn and H16. In comparison, W2-ALE also accumulated PHA better in nitrogen-limiting condition (20.1 %) than non-limiting (3.1 %). Nonetheless, maximum PHA titer was 138.6 ± 51.5 mg/L, less than what was seen with Sn+H16.

PHA composition in all consortia were identified by GC-FID (Fig. 3d). DMCs with *Pseudomonas* sp. accumulated medium chain length PHA (mclPHA) with C8, C10, and C12 as the dominant monomers. W2-ALE produced both short chain length PHA (sclPHA) and mclPHA, and all monomers from C4–12 were detected, with C8 dominance (33 %), followed by C10 (31 %), and C9 (13 %). H16 and its DMCs with Ap and Sn accumulated polyhydroxybutanoate (PHB) with C4 as the main monomer (91–95 %), and lower ratio of C5 (4–6 %). The monoculture of Sn exhibited a small peak in the GC chromatogram at the retention time corresponding to the C12 monomer. However, this peak was consistently observed across different analyses and experimental conditions; therefore, it is more likely attributable to esterification of other non-PHA cellular lipids rather than representing a true PHA monomer. The variation in monomer composition among different DMCs demonstrates the potential of defined consortia to tailor the synthesis of specific PHA types from the same starting substrate.

3.3. Effect of C/N on PHA production at high substrate concentration

Since the DMCs containing Sn showed an increase in PHA titer, they were subsequently tested with higher substrate concentration (10 g/L or 8.62 gC/L PO wax), shown to be inhibitory for microbial growth (particularly for single strains). C/N ratio had pronounced effects on PHA accumulation (Fig. 4). Cell biomass concentrations produced from high carbon feed (8.62 gC/L) were not significantly different in the mixed cultures, except for Sn+H16 and W2-ALE under C/N of 33 (NH_4Cl concentration of 1 g/L (0.26 gN/L)) (Fig. 4a). W2-ALE grew 1.6–4.2-fold better than DMCs at high substrate concentration, producing 2.4 ± 0.1 gCDW/L, as expected from the MMC enriched and adapted on PO wax [30]. This result highlights the advantage of ALE in training MMCs to utilize unconventional substrates.

On the other hand, in terms of PHA content per cell biomass, W2-ALE exhibited modest PHA accumulation at both C/N of 33 (8.8 ± 2.4 % per CDW) and C/N of 133 (13.9 ± 0.7 % per CDW) (Fig. 4b). DMCs Sn+H16 (22.9 ± 3.1 % per CDW) and Sn+*ΔlysR* (23.1 ± 0.6 % per CDW) showed 1.6–2.6-fold higher PHA accumulation than W2-ALE at their respective optimal C/N ratios at 133 and 33. This suggests that the designed synthetic mixed culture could possibly outcompete the natural microbial consortia in specific conditions, especially those that require a combination of specialized metabolic activities.

C/N ratio significantly affected the PHA titers of W2-ALE, Sn+*ΔlysR*, and Sn+H16. Both W2-ALE and Sn+*ΔlysR* preferred a lower C/N of 33, resulting in PHA titers of 207.9 ± 60.3 mg/L and 163.8 ± 12.6 mg/L, respectively. In contrast, Sn+H16 achieved its highest PHA titer at a higher C/N ratio of 133, reaching 192.6 ± 26.5 mg/L. Although W2-ALE exhibited the lowest PHA content per unit cell biomass, it produced the highest overall PHA titer among the tested consortia, thanks to the higher biomass titer.

It should be noted that Sn+H16 always accumulated high PHA (23.6 ± 1.0 % per CDW (Fig. 3C) and 22.9 ± 3.1 % per CDW (Fig. 4b)) only under the condition with low nitrogen concentration (0.065 gN/L), regardless of the carbon source concentration. Cell biomass concentrations from both low (1.96 gC/L, Fig. 3a) and high (8.62 gC/L, Fig. 4a) carbon feeds were also similar at 0.065 gN/L (accounting for C/N of 30 and 133, respectively), thus resulting in similar PHA titers (192.6 ± 26.5 and 193.0 ± 4.3 mg/L, respectively). This indicates that limiting nitrogen concentration limited PO wax utilization of Sn+H16 for both biomass and PHA production. While under higher nitrogen conditions (0.26 gN/L), cell biomass concentration at high PO wax increased 1.8-fold from low PO wax. Nevertheless, very low PHA accumulations (<2 % per CDW) were observed for both carbon levels.

In the current study, PHA was produced from PO pyrolysis wax as a sole carbon source, a hydrocarbon substrate mainly made of alkanes. PHA biosynthesis from hydrocarbons is initiated by aerobic degradation of alkanes, in which alkanes are sequentially oxidized to alkanols, alkanals, and ultimately alkanoic acids. Alkanoic acids will be further metabolized via β-oxidation [33,34]. Under nitrogen-replete conditions, β-oxidation is the catabolic pathway that converts alkanoic acids into acetyl-CoA, which subsequently enters central metabolism (TCA cycle) to support energy generation and biomass formation (producing essential carbon building blocks). Under nitrogen-limiting conditions, the intermediates from β-oxidation, specifically 2-*trans*- enoyl-CoA, are then converted to the PHA monomer (*R*)-3-hydroxyacyl-CoA by monomer-supplying enzymes 3-ketoacyl-ACP reductase (FabG) and (*R*)-specific enoyl-CoA hydratase (PhaJ), respectively. Ultimately, 3-ketoacyl-CoA will be converted to acetyl-CoA by 3-ketoacyl-CoA thiolase (FadA). In *C. necator* and other sclPHA accumulating organisms, two acetyl-CoA are then condensed by 3-ketothiolase (PhaA) and reduced by NADPH-dependent acetoacetyl-CoA reductase (PhaB), and PHA synthase (PhaC) to produce PHA [35,36]. *C. necator* H16 was reported to have six potential active 3-ketothiolases, including PhaA and BktB, which have a substrate specificity toward C4 and C4–6 monomers [37]. In this study, H16 or DMC with H16 as one of the members also showed to accumulate PHA with 94–95 % C4-monomer and 5–6 % C5-monomer from PO wax. Although the *Pseudomonas* species used in this study are known PHA producers from various substrates [16, 38–44], they exhibited lower PHA titer from PO wax (even though, in fact, GO16 and *ΔlysR* accumulated PHA at 6.9–7.7 % and 14.0–21.4 %

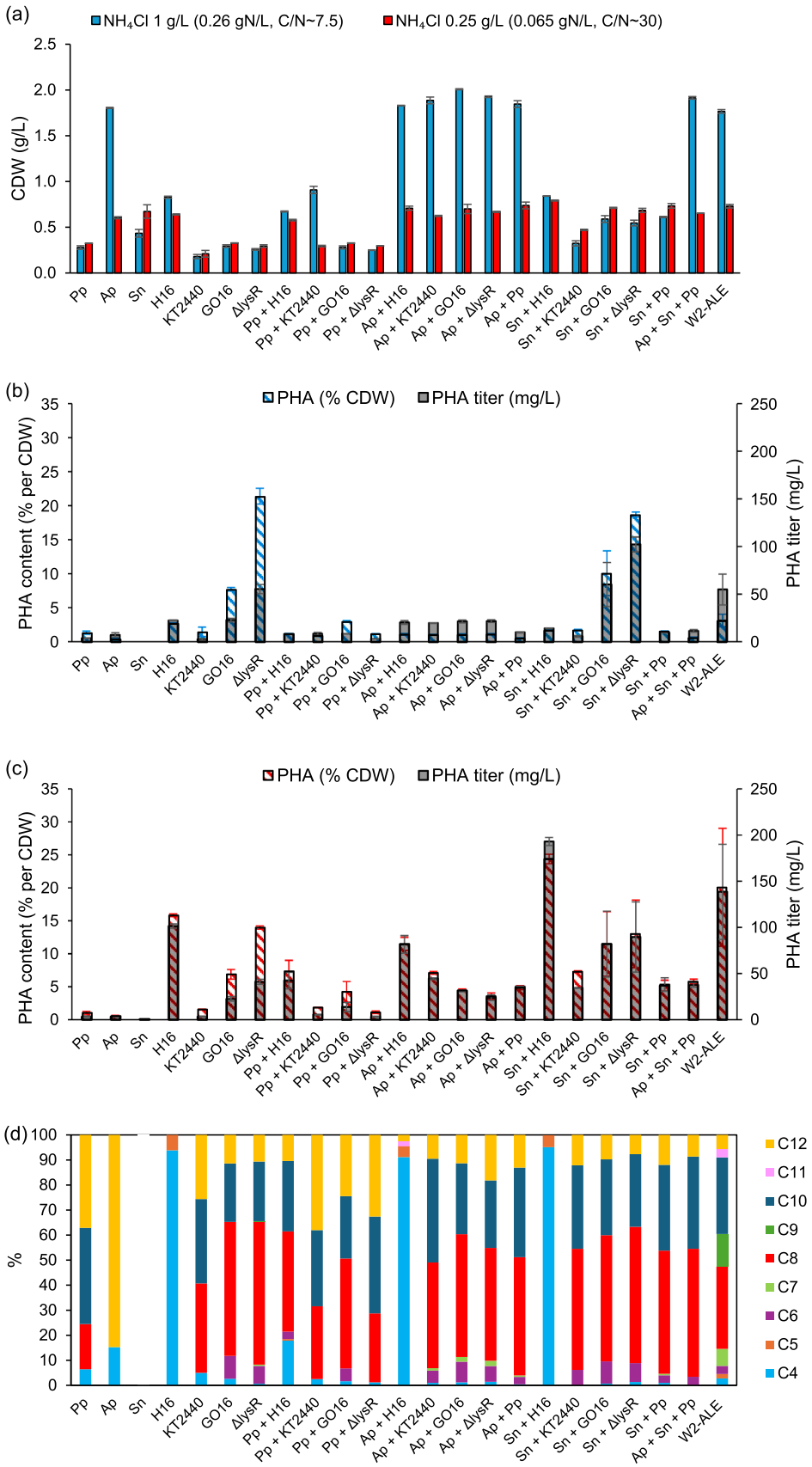

Fig. 3. Screening of DMCs in comparison with monocultures and MMC (W2-ALE) on PHA production: CDW (a), PHA content and PHA titer from the PHA fermentation at low PO wax (2.2 g/L or 1.86 gC/L) in nitrogen-non-limited (0.26 gN/L) (b) and limited (0.065 gN/L) (c) MSM, and PHA monomer distribution (d).

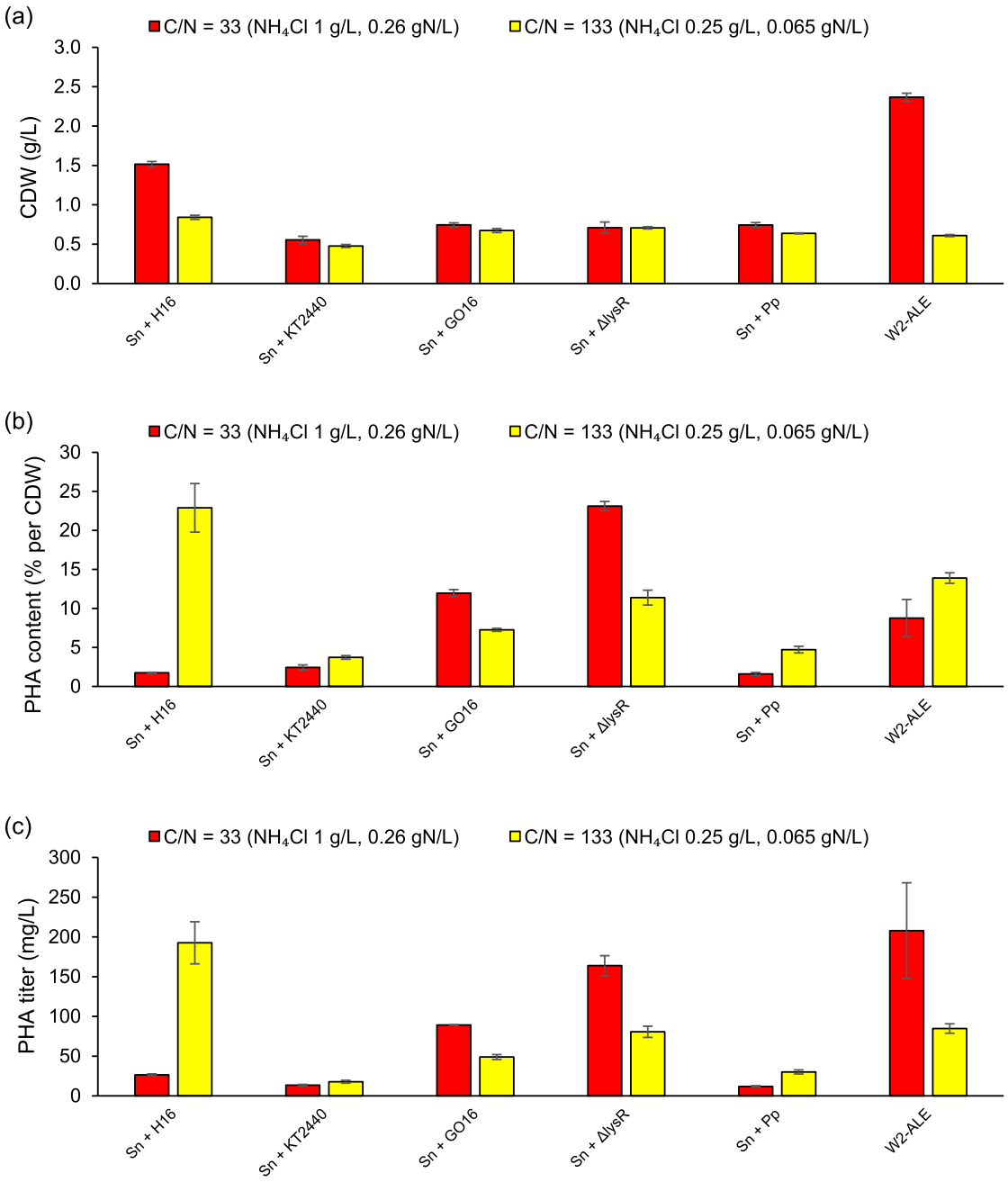

Fig. 4. PHA production by DMCs and MMC (W2-ALE) at high PO wax concentration (10 g/L or 8.62 gC/L) with C/N of 33 or 133: CDW (a), PHA content (b), and PHA titer (c).

PHA per CDW, respectively*)*. Pp, GO16, *ΔlysR,* and KT2440 all showed poor growth with PO wax when tested individually (Fig. 3a), suggesting they are not well equipped to deal with such substrate. Another reason might be related to substrate competition between various metabolic pathways. Alkanoic acids, the intermediate from alkane degradation, can be shuffled toward wax ester and triacylglycerol production in some bacteria, e.g., *Acinetobacter* sp., *Alcanivorax borkumensis, Marinobacter* sp., *Mycobacterium* sp., *Pseudomonas* sp., *Rhodococcus* sp., and *Streptomyces* sp., by a CoA-dependent acyltransferase enzyme known as wax ester synthase/diacylglycerol acyltransferase (WS/DGAT) [45,46]. This seems to be coherent with our previous study in which we observed substrate competition between neutral lipid and polyester biosynthesis pathways, resulting in lower PHA accumulation using a MMC process [30].

Sn, our most interesting isolate, was able to consume 27 % and 45 % PO wax in 24 and 48 h, respectively (Fig. S2). Gene annotation of the draft genome of *Serratia* sp. by RAST v2.0 revealed the presence of $FMNH_2$-dependent alkanesulfonate monooxygenases, which has similar sequence to *LadB* alkane monooxygenase and may be involved in alkane metabolism [47]. Genome mining to find *alkB*-like genes through homologous sequence search using BLAST showed that Sn possesses genes with sequence similarity to *alkB* of some *Pseudomonas, Brucella, Geobacillus*, and *Mycobacterium* species, although the similarities are generally low (Fig. S3). Gene annotation also showed that Sn has several genes involved in biosynthesis pathways of butanol, butyrate, lactate, acetoin, butanediol, and fatty acids, which are all reported to be suitable substrates for H16 [48]. This might partly explain the positive interaction between Sn and H16, observed in this study. Moreover, analysis of

the products from alkane biodegradation by Sn demonstrated that alkanoic acids of varying chain lengths were produced, corresponding to the alkanes supplied (Fig. S4). In principle, H16 could accumulate PHA from the oxidized compounds, especially alkanoic acids (carboxylic acids), derived from PO wax components metabolized by its own metabolism and those produced by Sn.

3.4. Optimizing PHA production in flask-scale

So far, the screening of mixed cultures for PHA production indicated that the DMC of Sn and H16 and adapted MMC (W2-ALE) were the most interesting consortia with the highest PHA accumulation. Therefore, process optimization was performed on these two consortia to maximize

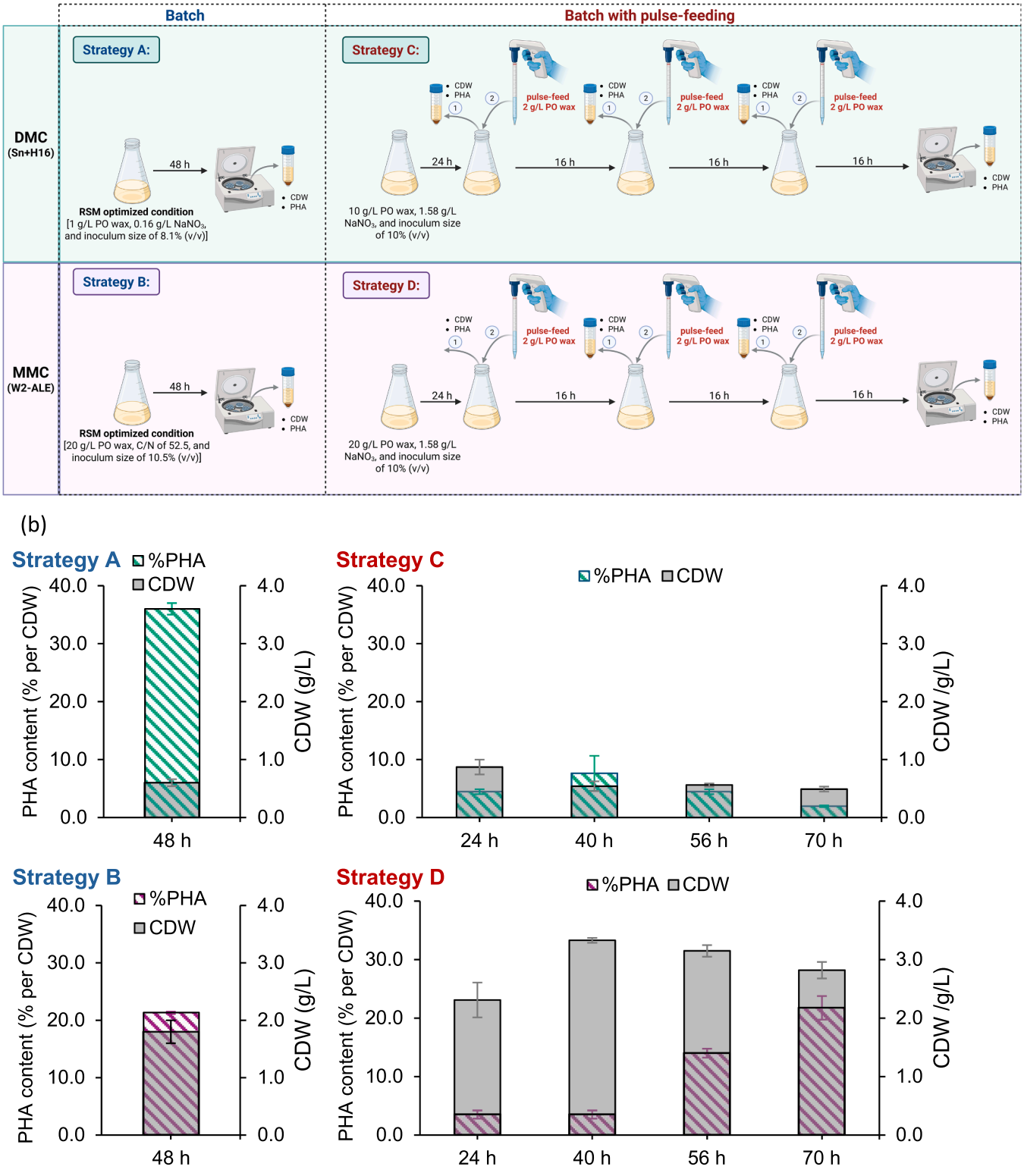

Fig. 5. Investigated fermentation strategies to improve PHA titer from PO wax; Strategy A (Sn+H16) and B (W2-ALE) are batch fermentations under statistically optimized conditions predicted by the models generated using Response Surface Methodology (RSM), and Strategy C (Sn+H16) and D (W2-ALE) are batch fermentations with pulse-feeding of PO wax (a). PHA production from each strategy: PHA content and CDW (b); and PHA titer (c).

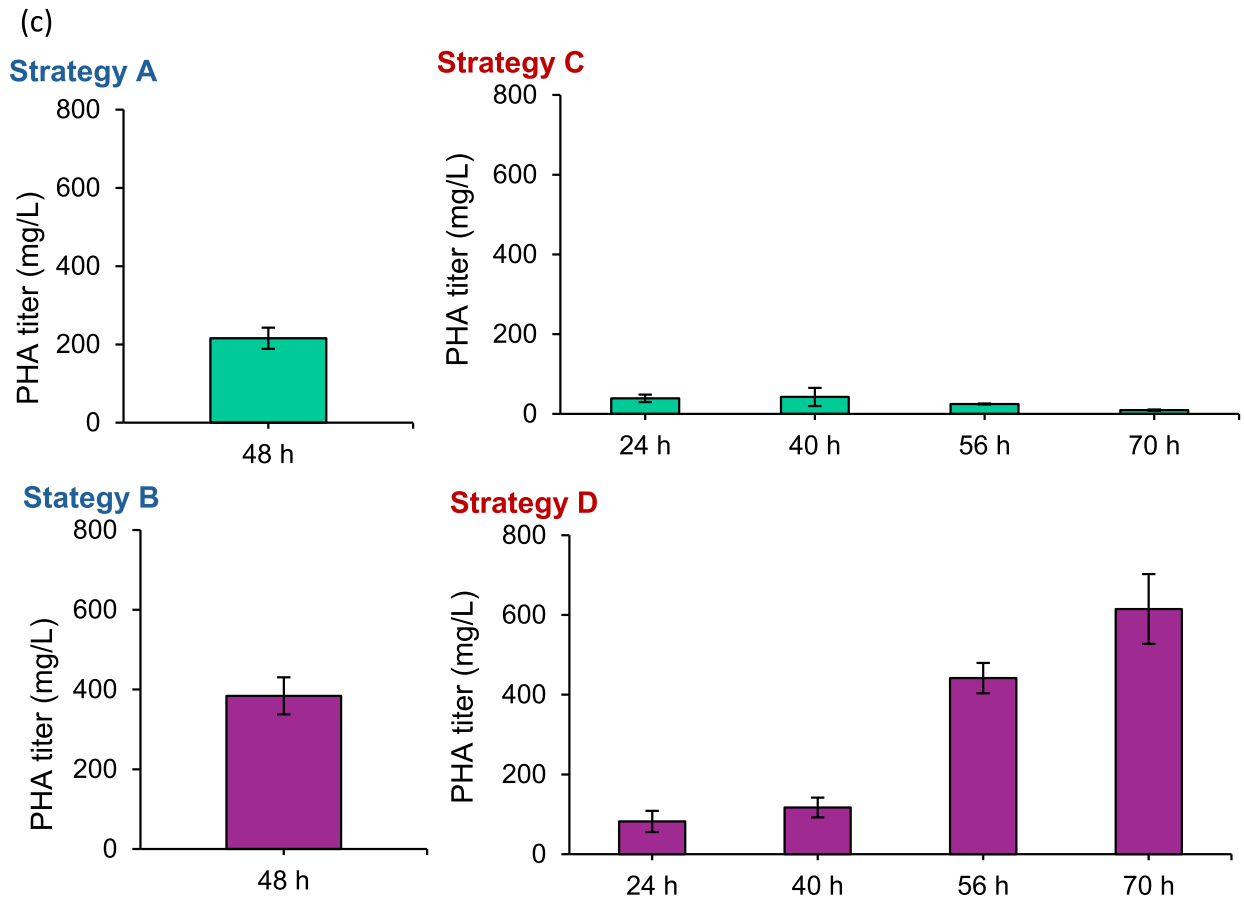

Fig. 5. (*continued*).

PHA titers.

Firstly, the effect of the nitrogen source on PHA production was investigated in shake-flask cultivation using a high PO wax concentration (10 g/L). Three common inorganic nitrogen forms, namely NH_4Cl, $NaNO_3$, and $NaNO_2$, were used to supply NH_4^+-N, NO_3^--N, and NO_2^--N at the concentration of 0.065 gN/L (nitrogen-limiting condition). NO_3^--N promoted the highest PHA titer for both Sn+H16 and W2-ALE, accounting for 22.7 % and 13.8 % higher than NH_4^+-N, respectively (Fig. S5). Whereas, NO_2^--N led to the lowest PHA production, showing almost no PHA accumulation in Sn+H16 and 3.6 % lower PHA production than NO_3^--N in W2-ALE. Accordingly, $NaNO_3$ was selected as the nitrogen source for the subsequent experiments.

Following nitrogen source selection, strategies to improve PHA titers were investigated in both Sn+H16 and W2-ALE using two approaches: 1) batch fermentation under statistically optimized conditions predicted by the models generated using Response Surface Methodology (RSM), and 2) batch fermentation with pulse-feeding of PO wax. The experimental design is illustrated in Fig. 5a as Strategy A, B, C, and D, where Strategies A and C correspond to PHA production by Sn+H16, and Strategies B and D correspond to PHA production by W2-ALE. Detailed discussions of each strategy are provided as following.

Strategy A: A three-factor three-level Central Composite Design (CCD) was employed to generate experimental data for constructing quadratic response surface models using RSM (Table S2 and Fig. S6). The models were used to predict the optimal combination of three parameters, including PO wax concentration, $NaNO_3$ concentration, and DMC inoculum size for maximizing PHA titer and yield. Batch fermentation using the optimal condition (1 g/L PO wax, 0.16 g/L $NaNO_3$, and inoculum size of 8.1 % v/v) resulted in a final PHA titer of 215.7 ± 27.1 mg/L (biomass production of 0.60 ± 0.06 gCDW/L and PHA content of 36.0 ± 1.0 % per CDW) after 48 h, which was only 12 % higher than the unoptimized condition (192.6 ± 26.5 mg/L). The slight increase in PHA titer was primarily attributed to an increase in intracellular PHA content (improved from 22.9 ± 3.1 % to 36.0 ± 1.0 % per CDW), rather than an increase in biomass titer. Moreover, model prediction, supported by experimental data, showed that PO wax concentrations higher than 1 g/L resulted in similar or slightly lower PHA titers; therefore, using 1 g/L PO wax yielded the highest PHA per substrate input.

Strategy B: The RSM-CCD optimization for W2-ALE process was previously conducted in our published study [30]. Batch fermentation using predicted optimal condition (20 g/L PO wax, a C/N ratio of 52.5, and inoculum size of 10.5 % v/v) resulted in a final PHA titer of 384.1 ± 46.5 mg/L (biomass production of 1.8 ± 0.2 gCDW/L and PHA content of 21.3 ± 0.2 % per CDW) after 48 h. This titer was 85 % higher than that obtained under the unoptimized condition (207.9 ± 60.3 mg/L).

Strategy C: Batch fermentation with pulse-feeding of PO wax was performed using Sn+H16 process, aiming to enhance PHA titer by increasing both cell biomass and PHA content. The first stage (growth phase) was conducted in batch mode for 24 h using an initial $NaNO_3$ concentration of 1.58 g/L (equivalent to 0.26 gN/L) and a high PO wax concentration of 10 g/L to ensure complete nitrogen consumption. After 24 h, a second stage (PHA production phase) was initiated by nitrogen depletion and pulse-feeding of PO wax at a concentration of 2 g/L thrice at the interval of 16 h to supply excess carbon. The pulse feed strategy was justified by the preliminary growth data from 24 h-batch cultivation in shake-flasks, where PO wax uptake rate was 0.167 g/L/h under nitrogen-non-limiting condition. At this rate, 2 g/L PO wax would theoretically be consumed within approximately 12 h; however, the feeding interval was extended to 16 h to account for the expected slower uptake rate owing to nitrogen depletion during this pulse-feed period. At 24 h, the biomass concentrations reached 0.87 ± 0.13 gCDW/L with low PHA accumulation (4.5 ± 0.4 % per CDW) (Fig. 5b). During the

subsequent pulse-feeding phase, Sn+H16 exhibited neither further growth nor PHA accumulation, and thus, the PHA production was deplenished using this strategy (final PHA titer at 72 h of 9.5 ± 1.6 mg/L) (Fig. 5c).

Strategy D: Batch fermentation with pulse-feeding of PO wax, similar to Strategy C, was performed using W2-ALE process. The first stage (growth phase) was performed in batch mode for 24 h using an initial $NaNO_3$ concentration of 1.58 g/L (equivalent to 0.26 gN/L) and a high PO wax concentration of 20 g/L. Higher PO wax concentration was used in this strategy, compared to Strategy C, because prior batch experiments illustrated that W2-ALE can utilize higher concentration of PO wax than Sn+H16. After 24 h, the PHA production stage was initiated by nitrogen depletion and pulse-feeding of PO wax at a concentration of 2 g/L thrice at the interval of 16 h to supply excess carbon, identical to Strategy C. At 24 h, the biomass concentrations reached 2.31 ± 0.30 gCDW/L (Fig. 5b). Following the first pulse feed, W2-ALE continued to grow, reaching a biomass concentration of 3.33 ± 0.04 gCDW/L at 40 h. It also demonstrated substantial PHA accumulation, increasing from 3.5 % to 21.8 % per CDW over the PHA production stage, resulting in the final PHA titer of 615.0 ± 87.6 mg/L at 72 h (Fig. 5c).

From Strategy A and B, statistical optimization of nutrient composition (carbon and nitrogen levels) was proven to improve the PHA titers in batch fermentation. However, bioprocess development by integrating pulse-feeding of the carbon source offered greater leverage and enabled improvement in production titers beyond what can be achieved in simple batch cultivation. Among 4 strategies, Strategy D resulted in the highest PHA titer (2.9, 1.6, and 64.7-fold higher than Strategy A, B, and C, respectively). Nevertheless, the PHA yield and productivity remained relatively low, at 0.024 ± 0.003 gPHA/gPOwax-added and 8.54 ± 1.22 mg/L/h, respectively. Therefore, the feeding scheme was further optimized in the following bioreactor-scale fermentations to improve overall process performance.

DMC (Sn+H16) exhibited less robustness and adaptability to dynamic environmental conditions than MMC (W2-ALE), most likely due to the changes in interspecies relationship upon the changes in operating conditions. Under batch fermentation with nitrogen limitation (Strategy A), Sn and H16 exhibited cooperative behavior, resulting in higher PHA production than that achieved by either monoculture alone. It was most likely that Sn converted hydrocarbons into carboxylic acids, which served as precursors for PHA biosynthesis by H16. In contrast, under batch fermentation with pulse-feeding (Strategy C), in which nitrogen was sufficient during the first stage, Sn may have overgrown or inhibited H16 during this phase, leading to a reduced H16 population and overall PHA production. To test this hypothesis, a separate experimental setup was conducted in which the colony-forming units (CFU) of Sn and H16 were monitored under nitrogen-non-limiting conditions. The results showed that H16 initially exhibited higher CFU counts than Sn during the first 8 h of cultivation; however, the CFU of H16 subsequently declined, in concurrence with the increase of Sn which finally outcompeted H16 (Fig. S7). This suggests that Sn may produce inhibitory compounds that suppress the growth of H16 under benign environment. In a previous study, secondary metabolite producing gene cluster analysis showed that *S. nematodiphila* MB307 had enterobactin, turnerbactin, ravidomycin, prodigiosin, and xantholipin producing clusters, which are siderophores and bioactive antibiotics used to gain competitive advantage and ecological fitness [49].

The interactions among microbial members in the artificially designed consortia do not arise naturally but instead occur under imposed conditions; consequently, these interactions may shift in response to environmental perturbations. Microbial members with less capacity to utilize available resources may be outcompeted, and poor growth of one member can destabilize or collapse the entire consortium [50]. This could explain what was observed with the Sn+H16 consortium in Strategy C, in which Sn may outcompete (and/or inhibit) H16 under nitrogen-sufficient condition; thus, the consortium was unable to resume PHA accumulation even after subsequent nitrogen depletion. A previous study from Ma et al. (2022) investigated the emergence of antagonistic relationship in an artificial co-culture of *Synechococcus elongatus cscB*$^{+}$ and engineered *Escherichia coli* (producing 3-hydroxypropionic acid from CO_2), which led to the population instability, through multi-omics analyses. They found that the competitive consumption of phosphorus and nitrogen between the microbial members could be the cause of population instability [51]. The strategies to minimize competition and establish cross-feeding between species are, therefore, essential for maintaining the stability of DMC. This often requires strain engineering (or co-evolution) to create metabolic interdependence or reduce nutrient competition among DMC members. For instance, in *P. putida-E. coli*consortium converting a mixture of glucose and xylose to mcl-PHA, gene knockout was performed on the *E. coli*s train to restrict its glucose utilization and thus reduce substrate competition with engineered *P. putida* [52]. Another study employed a nitrate-blind *P. putida* strain in a *S. elongatus–P. putida* consortium, enabling *S. elongatus* to grow and convert CO_2 to sucrose, used as a carbon source by *P. putida,* while creating nitrogen limitation for *P. putida* to enhance PHA accumulation [53]. This example shows that while DMC can achieve highly specialized and efficient production, their success relies on stringent regulation of community members or the use of engineered strains to ensure stable performance. In our present study, further bioprocess optimization on the DMC of Sn and H16 seems more challenging due to the instability of interspecies interactions, as discussed. Additional detailed studies on kinetics and cross-feeding mechanisms are required. Testing different Sn:H16 ratios, co-substrate feeding, or strain additions at different time intervals might possibly improve the DMC performance in a fed-batch process. Engineering of individual strains (i.e. to create metabolic interdependence) might even be needed to maintain a stable microbial relationship.

In contrast to naturally adapted mixed consortia, in which long-term co-evolution selects for complementary metabolisms and niche partitioning, metabolic interdependence emerges and strong cross-feeding interactions are sustained over the dynamic environmental conditions (i.e., affected by pulse-feeding in Strategy D in this study) [54,55]. In addition, high diversity and functional redundancy (typical characteristics of MMC) make them more robust and resilient, even though the microbial community composition is likely to vary in response to transient conditions. A properly enriched and stable functional consortium can be considered as a "superorganism". While the relative abundance of specific populations may shift throughout the process, the community maintains functional redundancy, where multiple taxonomically diverse species perform the same ecological function or metabolic task [56]. A previous study illustrated that the performance of PHA-storing MMC was not significantly different when the substrate was changed from molasse to cheese whey ($Y_{PHA/VFA}$ of 0.68 ± 0.09 and 0.80 ± 0.11 Cmol/Cmol, respectively), despite the shift in the community's population (from Actinobacteria-dominant to Firmicutes-dominant) [57]. Another study showed that operational conditions (e.g., organic loading rate and feeding regime) influenced the composition of the phototrophic mixed culture. Nevertheless, the presence of several PHA-producing genera, including *Rhodopseudomonas, Rhizobium, Hyphomicrobiaceae, Rhodobacter*, and *Chromatiaceae*, sustained PHA production (31 % gPHA/gVSS and 2.67 gPHA/L/d), even though these genera were enriched under different conditions. In particular, the first three genera were enriched at higher organic loading rates of fermented wastewater as a carbon source [58]. This underlines the greater robustness and functional stability of adapted MMC compared to assembled DMC (bottom-up approach) as a biocatalyst in bioprocesses.

3.5. *Fed-batch with hybrid feeding strategy to improve PHA production by MMC (W2-ALE) process in bioreactor-scale*

To improve PHA yield and productivity of the process based on Strategy D, fed-batch PHA production was optimized in a multi-parallel bioreactor system, using a hybrid feeding strategy. The optimized

process was carried out in 4 phases: 1) initial batch phase (0–8 h), 2) exponential feeding phase (8–24 h), 3) pulse feeding phase (24–80 h), and 4) final prolonged batch phase (80–96 h). The first two phases were performed under nitrogen-non-limiting-condition, aiming to accumulate microbial biomass, while the latter two phases were performed under nitrogen-limiting conditions to enhance PHA accumulation. The feed tank for exponential feeding contained 10 g/L PO wax and 1.58 g/L $NaNO_3$ (C/N of 33), while the one for pulse feeding contained 20 g/L PO wax and 0.39 g/L $NaNO_3$ (C/N of 265). The feeding scheme is shown in Fig. 6.

Preliminary batch cultivation was performed to collect data about growth profile and specific growth rate of W2-ALE on PO wax. As PO wax is composed of a mixture of alkanes and alkenes of different chain lengths [30], diauxic growth was observed. Therefore, the average specific growth rate (μ_{avg}) was used instead of maximum specific growth rate (μ_{max}) for exponential feeding rate calculation. Experimental μ_{avg} of 0.278 h^{-1} was observed. However, 75 % of experimental μ_{avg} was used as a set constant growth rate ($\mu_{constant} = 0.209\ h^{-1}$) for the exponential feeding in this study to prevent substrate overfeeding. The first 8 h were operated as a batch (initial volume of 278 mL) to start up the reactor and cultivate the consortium until reaching early log phase, when the cell biomass reached 0.83 ± 0.25 gCDW/L. Then, the exponential feeding was started, maintaining $\mu_{constant}$ at 0.209 h^{-1} by feeding increased amounts of PO wax as shown in Fig. 6. Exponential feeding of 10 g/L PO wax to the bioreactor led to an accumulated volume of almost 600 mL after 20 h; thus, the feeding was stopped to allow for spare working volume, needed for pulse feeding during the following PHA production phase. At 24 h, the biomass accumulation achieved 3.59 ± 0.95 gCDW/L without high PHA accumulation (4.0 ± 1.8 % per CDW), while the nitrogen was depleted (6.4 ± 2.0 mgNO_3-N/L) (Fig. 7a).

At this point, the cultivation mode was switched from cell accumulation to PHA production phase, using pulse feeding of 20 g/L PO wax stock solution with limiting nitrogen concentration (0.065 gN/L). The PO wax and nitrogen concentration in the bioreactor at each pulse were 1 g/L and 0.0033 gN/L, respectively. PO wax was maintained at a low concentration (1 g/L) during pulse feeding, as preliminary results showed the highest PHA content in this condition (Table S3). Thus, pulsing higher amounts of PO wax did not enhance PHA accumulation and even ceased PHA production, likely due to hydrophobic substrate accumulation that eventually inhibited oxygen transfer and caused cell death. Therefore, the pulse-feeding interval was instead optimized to improve PHA productivity (Fig. S8). Moreover, hydrophobic hydrocarbons were reported to accumulate in the lipid bilayer membrane of microorganisms, affecting membrane structure, integrity, and fluidity, as well as the membrane-embedded proteins [59]. This might interfere with the hydrophobic substrate uptake itself. The optimized pulse feed was performed every 2 h interval from 24 to 44 h of cultivation time, afterward switching to 6 h intervals from 44 to 80 h. Switching pulse feeding interval to 6 h maintained PHA production at 17–19 %. A drop of PHA content from 17 % (at 44 h) to 11 % per CDW (at 48 h until the end of feeding period) was observed in preliminary test when using pulse feeding interval at 2 h throughout the entire PHA accumulation phase (Fig. S8). The fast feeding rate rapidly increased the reactor volume and caused cell dilution, while simultaneously increasing the concentration of hydrophobic PO wax in the bioreactor. This likely imposed stress on the cells (e.g., substrate toxicity and limited oxygen transfer), driving them into a maintenance metabolism in which stored PHA was utilized as an energy source [60]. Switching pulse feeding interval from every 2 h to 6 h at the right time prevented cell dilution by keeping the dilution rate (D) lower than the specific growth rate (μ); thus, maintaining PHA content (Fig. S9). The cultivation was prolonged until 96 h after the feeding was stopped at 80 h, resulting in a further increase in PHA content from 18.0 ± 0.5 to 22.1 ± 0.9 % per CDW and a final PHA titer of 772.1 ± 93.3 mg/L (the average titer was calculated from 4 replicates, data of each replicate are shown in Table S4). This result indicates that the residual PO wax was gradually used for PHA synthesis again once the transient condition due to fed-batch feeding was terminated. PHA titer achieved in this study was higher than reported titers from similar hydrocarbon mixture substrates, such as crude oil and bilge waste (147–300 mg/L) [61,62]. The biomass concentration during PHA production phase was relatively stable, due to the increase of reactor working volume by >50 % that counterbalanced the cell growth. Mixed PHA were produced with C8, C9, and C10 as the dominant monomers (23 %, 13 %, and 34 %, respectively, Table S4).

Biomass and PHA yields were calculated based on the total mass of PO wax fed into the bioreactors. This is because the PO wax emulsion became unstable during fermentation, leading to wax partially agglomerating, which interfered with proper extraction for the substrate analysis, potentially leading to misinterpretations of actual PO wax consumption. A total PO wax of 19.7 g (equivalent to 15.9 g/$L_{final\ volume}$) was fed to the bioreactors, resulting in final biomass and PHA yield at 96 h of 0.17 ± 0.02 gBiomass/gPOwax-added and 0.048 ± 0.006 gPHA/gPOwax-added, respectively (Fig. 7b). The biomass yield was highest in the first 24 h during biomass production phase (0.48 ± 0.04 gBiomass/gPOwax-added) but gradually declined afterward as the process transitioned into the PHA accumulation phase, where the community stopped growing due to nitrogen depletion. In contrast, PHA yield increased and became relatively stable during 50–96 h (0.045–0.049 gPHA/gPOwax-added). The PHA yield was 2-times higher than what observed in flask-scale fermentation. Overall, using non-

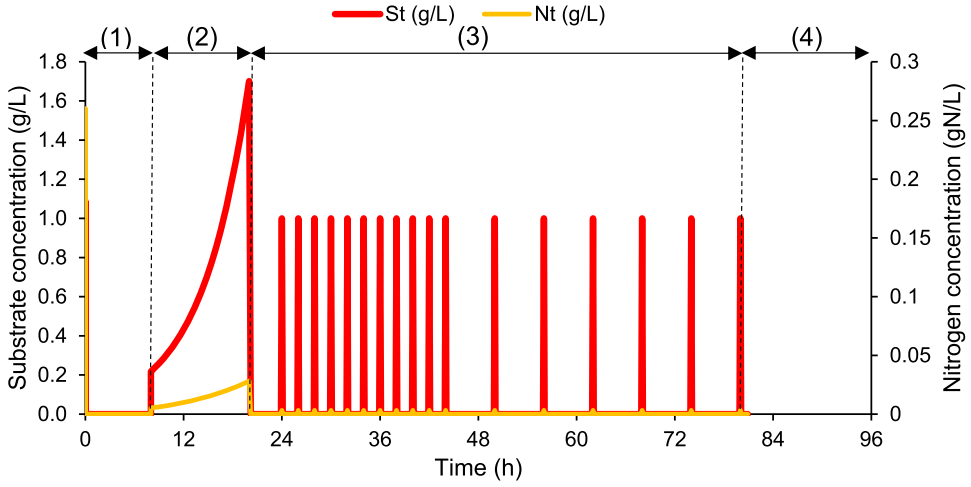

Fig. 6. Feeding regime of fed-batch fermentations with hybrid feeding, carried out in 4 phases: (1) initial batch phase, (2) exponential feeding phase under nitrogen-non-limiting condition, (3) pulse feeding phase under nitrogen-limiting condition, and (4) final prolonged batch phase.

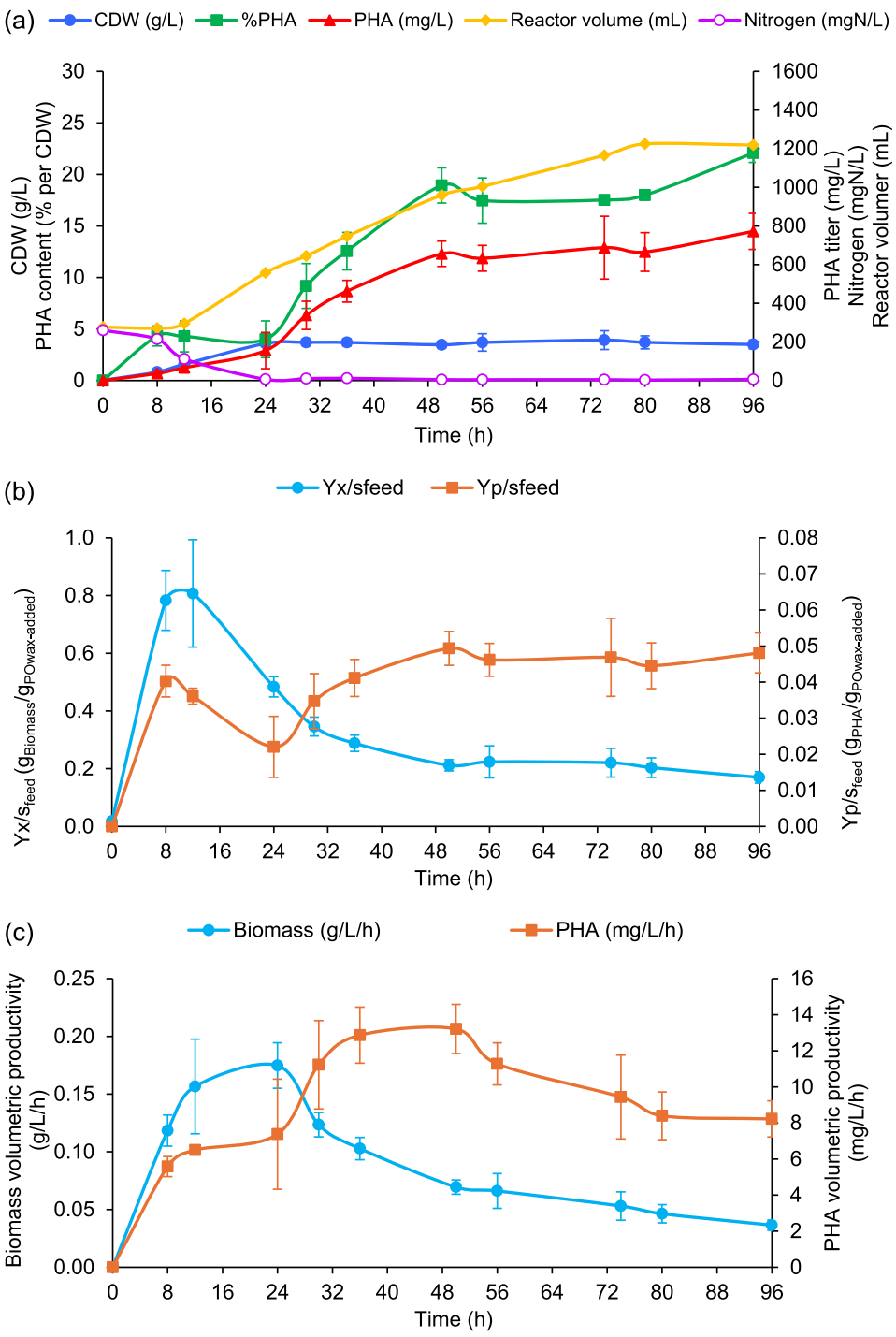

Fig. 7. Process performance of fed-batch fermentation with hybrid feeding by MMC (W2-ALE). CDW, PHA content, PHA titer, nitrogen concentration and reactor volume (a); Biomass and PHA yield per supplied PO wax (b); Biomass and PHA volumetric productivity (c).

oxidized PO wax as a carbon substrate for PHA production suffered from low PHA yield, as also reported by Guzik et al. (2014) using polyethylene (PE) wax resulting in a maximum PHA yield of 0.004 gPHA/gPEwax in batch fermentation [63].

In the present study, the highest PHA productivity was observed during 30–56 h (11.2–13.2 mg/L/h) but slightly decreased afterward during 56–96 h (8.2–9.4 mg/L/h) (Fig. 7c). The low concentration of PO wax in the substrate reservoir (for proper emulsion) necessitated a higher volume of feed, which contributed to reduced overall productivity. To improve the process performance, increasing the hydrophilicity of PO wax could facilitate the preparation of emulsions with higher substrate concentrations and allow smaller feed volumes to be added in the fed-batch process to achieve the same substrate input, thereby reducing changes or interferences in the fermentation environment. In addition, given that both PHA yield and productivity peaked around 50–56 h, reducing the total fermentation time and implementing different operating mode such as semi-continuous fermentation might improve the overall yield and productivity. The maximum productivity achieved in this bioreactor-scale fed-batch fermentation was 55 % higher than that of flask-scale.

4. Conclusions and future perspectives

This work demonstrates a tandem process by combining thermochemical-biotechnological approach for upcycling post-consumer PO to bioplastic PHAs. PO pyrolysis wax, representing a low-value by-product from real plastic waste pyrolysis process, was used directly as a substrate without additional pretreatment. Microbial consortia capable of accumulating PHA from PO wax were developed through two different approaches, including top-down engineering by enrichment and ALE of microbial community from plastic-contaminated soil and bottom-up engineering by co-culturing PO wax-degrading isolates with PHA-producing strains. In batch fermentation under nitrogen-limiting condition, MMC (W2-ALE) and DMC of Sn and H16 achieved the highest PHA titer among all screened microbial consortia (138.6 ± 51.5 mg/L and 193.0 ± 4.3, respectively). Applying statistically optimized condition to batch fermentation in the Sn+H16 process improved the PHA titer by only 12 %, and employing fed-batch fermentation even resulted in a decrease in PHA titer. This indicated that the interspecies relationship between Sn and H16 did not remain positive when changing fermentation conditions or operation modes, resulting in the loss of PHA producing ability. In contrast, the MMC process could be further optimized to increase PHA titer, illustrating the robustness of co-evolved microbial communities. Besides statistical optimization of cultivation parameters, which improved the PHA titer by 2.8-fold, bioprocess optimization was proven to be an important strategy for improving PHA production directly from non-oxidized PO wax without any co-substrate feeding. Using fed-batch fermentation with a refined advanced feeding strategy, the PHA titer of 772.1 ± 93.9 mg/L was achieved, showing 5.6-fold higher performance than initial flask-scale batch fermentation. Maximum PHA productivity was observed during 30–56 h at 11.2–13.6 mg/L/h but decreased afterward. The titer and productivity achieved in this study were the highest compared to what previously reported on non-oxidized PO wax. Future work should aim to further enhance and sustain productivity throughout the operating time (beyond the 50 h) to improve the process efficiency. This could be done, for instance, by 1) improving substrate solubility/availability and 2) implementing a semi-continuous process with repeated cycles of cell accumulation and PHA production phases. To improve substrate availability, pretreatment of PO wax (for instance, by using advanced oxidation processes (AOPs)) could be performed to improve emulsion stability and facilitate higher feedstock loadings. Additionally, developing thermophilic MMCs could facilitate bioconversion near the PO wax melting point (approximately 60 °C, thereby enhancing substrate accessibility and accelerating process kinetics.

MMC exhibits superior performance in degrading complex residue streams, such as the PO wax used in this study, by leveraging synergistic metabolic pathways and inherent functional redundancy. This allows them to break down heterogenous feedstocks while maintaining greater stability against environmental fluctuations. MMC process is a promising strategy for processing actual plastic pyrolysis waste streams, where fluctuations in feedstock composition are expected. In our previous work, which described the adaptive laboratory evolution strategy used to develop W2-ALE (the MMC used in this study), two distinct batches of PO wax from the commercial pyrolysis process were evaluated [30]. The first batch comprised 75 % alkanes, 22 % alkenes, 4 % aromatics, whereas the second batch contained 92 % alkanes, 7.8 % alkenes, 0.2 % aromatics. In addition, the hydrocarbon distribution in the second batch showed a higher proportion of long-chain compounds (C26–C39) compared to the first batch. Despite these variations, W2-ALE demonstrated robustness and was able to utilize both PO wax batches. Future studies should evaluate a broader range of industrial PO wax samples, which are expected to vary in aliphatic and aromatic hydrocarbon composition due to fluctuations in plastic waste feedstock in real-world pyrolysis processes, in order to further assess process robustness. Foreseen challenges are plastic additives, especially the organic additives that contain heteroatoms (e.g., N, S, Cl, Br) or metals/metalloids (e.g., Fe, Cu, Cr, Si) [64], which may contaminate the pyrolysis wax and negatively affect its biodegradability if present at sufficiently high concentrations. Moreover, high volatile aromatic hydrocarbons (BTEX) content in pyrolysis wax may exert inhibitory effects on microbial growth. In such case, the MMC may require further adaptation to BTEX or bioaugmentation with specialized BTEX-degrading strains. In principle, this should allow overcoming potential inhibition problems, also because the amount of additives used in POs is relatively modest (usually around few %) compared to other plastic types.

CRediT authorship contribution statement

Passanun Lomwongsopon: Writing – review & editing, Writing – original draft, Visualization, Supervision, Methodology, Investigation, Data curation, Conceptualization. **Tanja Narančić:** Supervision, Methodology. **Reeta Davis:** Methodology. **Meg Walsh:** Methodology. **Kevin E. O'Connor:** Investigation. **Cristiano Varrone:** Writing – review & editing, Supervision, Resources, Project administration, Investigation, Funding acquisition, Conceptualization.

Declaration of competing interest

The authors declare that they have no known competing financial interests or personal relationships that could have appeared to influence the work reported in this paper.

Acknowledgements

This work was supported by H2020 UPLIFT project [Grant Agreement no 953073], HORIZON Innovation Actions UPCYCLE [Grant Agreement no 101178389], and Carlsberg foundation [Grant no CF23-1685]. The authors wish to thank WPU Denmark and Anders Egede Daugaard from Technical University of Denmark for the supply of PO wax. The authors are also thankful to Kate Jounghyun Um for supplying *Pseudomonas umsongensis* GO16 and GO16 *ΔlysR*.

Supplementary materials

Supplementary material associated with this article can be found, in the online version, at doi:10.1016/j.polymdegradstab.2026.112148.

Data availability

Data will be made available on request.

References

[1] M. Steilemann, It's time to shift to net-zero emissions plastics, World Econ. Forum. (2022). https://www.weforum.org/agenda/2022/01/it-s-time-to-shift-to-net-zero-emissions-plastics/(accessed. August 12, 2024.
[2] H. Ritchie, How much of global greenhouse gas emissions come from plastics? Our World. Data. (2023). https://ourworldindata.org/ghg-emissions-plastics. accessed August 12, 2024.
[3] OECD, Global Plastics Outlook: Economic Drivers, Environmental Impacts and Policy Options, OECD Publishing, Paris, 2022, https://doi.org/10.1787/de747aef-en.
[4] PlasticsEurope, Plastics—The Facts 2022. https://plasticseurope.org/knowledge-hub/plastics-the-facts-2022/, 2022 accessed August 13, 2024.
[5] OECD, Global Plastics Outlook: Policy Scenarios to 2060, OECD Publishing, Paris, 2022, https://doi.org/10.1787/AA1EDF33-EN.
[6] M. Roux, C. Varrone, Assessing the economic viability of the plastic biorefinery concept and its contribution to a more circular plastic sector, Polymers 13 (2021) 3883, https://doi.org/10.3390/POLYM13223883. Vol.Page 3883 13 (2021).
[7] M.N. Omar, M.M. Minggu, N.A. Nor Muhammad, P.M. Abdul, Y. Zhang, A. B. Ramzi, Towards consolidated bioprocessing of biomass and plastic substrates for semi-synthetic production of bio-poly(ethylene furanoate) (PEF) polymer using omics-guided construction of artificial microbial consortia, Enzyme Microb. Technol. 177 (2024) 110429, https://doi.org/10.1016/J.ENZMICTEC.2024.110429.

[8] T. Tiso, T. Narancic, R. Wei, E. Pollet, N. Beagan, K. Schröder, A. Honak, M. Jiang, S.T. Kenny, N. Wierckx, R. Perrin, L. Avérous, W. Zimmermann, K. O'Connor, L. M. Blank, Towards bio-upcycling of polyethylene terephthalate, Metab. Eng. 66 (2021) 167–178, https://doi.org/10.1016/J.YMBEN.2021.03.011.

[9] F. Cerrone, B. Zhou, A. Mouren, L. Avérous, S. Conroy, J.C. Simpson, K. E. O'Connor, T. Narancic, Pseudomonas umsongensis GO16 as a platform for the in vivo synthesis of short and medium chain length polyhydroxyalkanoate blends, Bioresour. Technol. 387 (2023) 129668, https://doi.org/10.1016/J.BIORTECH.2023.129668.

[10] N. Zhang, M. Ding, Y. Yuan, Current advances in biodegradation of polyolefins, Microorganisms 10 (2022) 1537, https://doi.org/10.3390/MICROORGANISMS10081537. Vol.Page 1537 10 (2022).

[11] T. Oiffer, F. Leipold, P. Süss, D. Breite, J. Griebel, M. Khurram, Y. Branson, E. de Vries, A. Schulze, C.A. Helm, R. Wei, U.T. Bornscheuer, Chemo-enzymatic depolymerization of functionalized low-molecular-weight polyethylene, Angew. Chem. Int. Ed. 63 (2024) e202415012, https://doi.org/10.1002/ANIE.202415012;WGROUP:STRING:PUBLICATION.

[12] PlasticsEurope, Plastics – the fast Facts 2024. https://plasticseurope.org/knowledge-hub/plastics-the-fast-facts-2024/, 2024 accessed December 4, 2024.

[13] Y. Liu, K. Chandra Akula, K. Phani Raj Dandamudi, Y. Liu, M. Xu, A. Sanchez, D. Zhu, S. Deng, Effective depolymerization of polyethylene plastic wastes under hydrothermal and solvothermal liquefaction conditions, Chem. Eng. J. 446 (2022) 137238, https://doi.org/10.1016/J.CEJ.2022.137238.

[14] T. Lu, K. Jan, W.T. Chen, Hydrothermal liquefaction of pretreated polyethylene-based ocean-bound plastic waste in supercritical water, J. Energy Inst. 105 (2022) 282–292, https://doi.org/10.1016/J.JOEI.2022.10.003.

[15] L. Gan, Z. Dong, H. Xu, H. Lv, G. Liu, F. Zhang, Z. Huang, Beyond conventional degradation: catalytic solutions for polyolefin upcycling, CCS Chem. 6 (2024) 313–333, https://doi.org/10.31635/CCSCHEM.023.202303538.

[16] M.W. Guzik, T. Nitkiewicz, M. Wojnarowska, M. Sołtysik, S.T. Kenny, R.P. Babu, M. Best, K.E. O'Connor, Robust process for high yield conversion of non-degradable polyethylene to a biodegradable plastic using a chemo-biotechnological approach, Waste Manag. 135 (2021) 60–69, https://doi.org/10.1016/J.WASMAN.2021.08.030.

[17] C. Kourmentza, J. Plácido, N. Venetsaneas, A. Burniol-Figols, C. Varrone, H. N. Gavala, M.A.M. Reis, Recent advances and challenges towards sustainable polyhydroxyalkanoate (PHA) production, Bioengineering 4 (2017) 55, https://doi.org/10.3390/BIOENGINEERING4020055. Vol.Page 55 4 (2017).

[18] G. Corti Monzón, G. Bertola, M.K. Herrera Seitz, S.E. Murialdo, Exploring polyhydroxyalkanoates biosynthesis using hydrocarbons as carbon source: a comprehensive review, Biodegradation 2024 (2024) 1–20, https://doi.org/10.1007/S10532-023-10068-9.

[19] H. Park, H. He, X. Yan, X. Liu, N.S. Scrutton, G.Q. Chen, PHA is not just a bioplastic!, Biotechnol. Adv. 71 (2024) 108320, https://doi.org/10.1016/J.BIOTECHADV.2024.108320.

[20] European Commission, Waste framework directive, Eur. Comission. (2022) 3–30. https://environment.ec.europa.eu/topics/waste-and-recycling/waste-framework-directive_en. accessed September 28, 2022.

[21] C. Varrone, G. Floriotis, T.M.B. Heggeset, S.B. Le, S. Markussen, I.V. Skiadas, H. N. Gavala, Continuous fermentation and kinetic experiments for the conversion of crude glycerol derived from second-generation biodiesel into 1,3 propanediol and butyric acid, Biochem. Eng. J. 128 (2017) 149–161, https://doi.org/10.1016/J.BEJ.2017.09.012.

[22] S.K. Bhatia, R.K. Bhatia, Y.K. Choi, E. Kan, Y.G. Kim, Y.H. Yang, Biotechnological potential of microbial consortia and future perspectives, Crit. Rev. Biotechnol. 38 (2018) 1209–1229, https://doi.org/10.1080/07388551.2018.1471445.

[23] K. Jawed, S.S. Yazdani, M.A. Koffas, Advances in the development and application of microbial consortia for metabolic engineering, Metab. Eng. Commun. 9 (2019) e00095, https://doi.org/10.1016/J.MEC.2019.E00095.

[24] A. Burniol-Figols, C. Varrone, A.E. Daugaard, S.B. Le, I.V. Skiadas, H.N. Gavala, Polyhydroxyalkanoates (PHA) production from fermented crude glycerol: study on the conversion of 1,3-propanediol to PHA in mixed microbial consortia, Water Res. 128 (2018) 255–266, https://doi.org/10.1016/J.WATRES.2017.10.046.

[25] R. Moita Fidalgo, J. Ortigueira, A. Freches, J. Pelica, M. Gonçalves, B. Mendes, P. C. Lemos, Bio-oil upgrading strategies to improve PHA production from selected aerobic mixed cultures, N. Biotechnol. 31 (2014) 297–307, https://doi.org/10.1016/J.NBT.2013.10.009.

[26] F. Massot, N. Bernard, L.M.M. Alvarez, M.M. Martorell, W.P. Mac Cormack, L.A. M. Ruberto, Microbial associations for bioremediation. What does "microbial consortia" mean? Appl. Microbiol. Biotechnol. 106 (2022) 2283–2297, https://doi.org/10.1007/S00253-022-11864-8, 7 106 (2022).

[27] I. Corrado, C. Petrillo, R. Isticato, A. Casillo, M.M. Corsaro, G. Sannia, C. Pezzella, The power of two: an artificial microbial consortium for the conversion of inulin into polyhydroxyalkanoates, Int. J. Biol. Macromol. 189 (2021) 494–502, https://doi.org/10.1016/J.IJBIOMAC.2021.08.123.

[28] I. Radecka, V. Irorere, G. Jiang, D. Hill, C. Williams, G. Adamus, M. Kwiecień, A. A. Marek, J. Zawadiak, B. Johnston, M. Kowalczuk, Oxidized polyethylene wax as a potential carbon source for PHA production, Materials 9 (2016) 367, https://doi.org/10.3390/ma9050367.

[29] G. Welsing, B. Wolter, H.M.T. Hintzen, T. Tiso, L.M. Blank, Upcycling of hydrolyzed PET by microbial conversion to a fatty acid derivative, Methods Enzymol. 648 (2021) 391–421, https://doi.org/10.1016/bs.mie.2020.12.025.

[30] P. Lomwongsopon, T. Narancic, R. Wimmer, C. Varrone, Combined thermochemical-biotechnological approach for the valorization of polyolefins into polyhydroxyalkanoates: development of an integrated bioconversion process by microbial consortia, Chemosphere 367 (2024) 143671, https://doi.org/10.1016/J.CHEMOSPHERE.2024.143671.

[31] R.S. Peixoto, A.B. Vermelho, A.S. Rosado, Petroleum-degrading enzymes: bioremediation and new prospects, Enzyme Res. 2011 (2011) 475193, https://doi.org/10.4061/2011/475193.

[32] F. Abbasian, R. Lockington, M. Mallavarapu, R. Naidu, A comprehensive review of aliphatic hydrocarbon biodegradation by bacteria, Appl. Biochem. Biotechnol. 176 (2015) 670–699, https://doi.org/10.1007/S12010-015-1603-5.

[33] J.M. Jeon, S.J. Park, Y.S. Son, Y.H. Yang, J.J. Yoon, Bioconversion of mixed alkanes to polyhydroxyalkanoate by Pseudomonas resinovornas: upcycling of pyrolysis oil from waste-plastic, Polymers 14 (2022) 2624, https://doi.org/10.3390/POLYM14132624/S1.

[34] E.O. Fenibo, R. Selvarajan, A.L.K. Abia, T. Matambo, Medium-chain alkane biodegradation and its link to some unifying attributes of alkB genes diversity, Sci. Total Environ. 877 (2023) 162951, https://doi.org/10.1016/J.SCITOTENV.2023.162951.

[35] S.J. Park, J. Choi Il, S.Y. Lee, Engineering of *Escherichia coli* fatty acid metabolism for the production of polyhydroxyalkanoates, Enzyme Microb. Technol. 36 (2005) 579–588, https://doi.org/10.1016/J.ENZMICTEC.2004.12.005.

[36] A. Hiroe, M.F. Chek, T. Hakoshima, K. Sudesh, S. Taguchi, A. Hiroe, S Taguchi, M. F. Chek, T Hakoshima, K. Sudesh, Synthesis of polyesters III: acyltransferase as catalyst, (2019) 199–231. https://doi.org/10.1007/978-981-13-3813-7_7.

[37] H. Arikawa, S. Sato, Impact of various β-ketothiolase genes on PHBHHx production in Cupriavidus necator H16 derivatives, Appl. Microbiol. Biotechnol. 106 (2022) 3021–3032, https://doi.org/10.1007/S00253-022-11928-9/TABLES/8.

[38] S.T. Kenny, J.N. Runic, W. Kaminsky, T. Woods, R.P. Babu, K.E. O'Connor, Development of a bioprocess to convert PET derived terephthalic acid and biodiesel derived glycerol to medium chain length polyhydroxyalkanoate, Appl. Microbiol. Biotechnol. 95 (2012) 623–633, https://doi.org/10.1007/S00253-012-4058-4/TABLES/3.

[39] S. Yang, S. Li, X. Jia, Production of medium chain length polyhydroxyalkanoate from acetate by engineered Pseudomonas putida KT2440, J. Ind. Microbiol. Biotechnol. 46 (2019) 793–800, https://doi.org/10.1007/S10295-019-02159-5/TABLES/3.

[40] Y. Liu, S. Yang, X. Jia, Construction of a "nutrition supply–detoxification" coculture consortium for medium-chain-length polyhydroxyalkanoate production with a glucose–xylose mixture, J. Ind. Microbiol. Biotechnol. 47 (2020) 343–354, https://doi.org/10.1007/S10295-020-02267-7.

[41] I. Poblete-Castro, C. Aravena-Carrasco, M. Orellana-Saez, N. Pacheco, A. Cabrera, J.M. Borrero-de Acuña, Engineering the osmotic State of Pseudomonas putida KT2440 for efficient cell disruption and downstream processing of poly(3-Hydroxyalkanoates), Front. Bioeng. Biotechnol. 8 (2020) 517566, https://doi.org/10.3389/FBIOE.2020.00161/BIBTEX.

[42] M. Ai, Y. Zhu, X. Jia, Recent advances in constructing artificial microbial consortia for the production of medium-chain-length polyhydroxyalkanoates, World J. Microbiol. Biotechnol. 37 (2021) 1–14, https://doi.org/10.1007/S11274-020-02986-0/TABLES/2.

[43] M.W. Guzik, G.F. Duane, S.T. Kenny, E. Casey, P. Mielcarek, M. Wojnarowska, K. E. O'Connor, A polyhydroxyalkanoates bioprocess improvement case study based on four fed-batch feeding strategies, Microb. Biotechnol. 15 (2022) 996–1006, https://doi.org/10.1111/1751-7915.13879.

[44] T. Narancic, M. Salvador, G.M. Hughes, N. Beagan, U. Abdulmutalib, S.T. Kenny, H. Wu, M. Saccomanno, J. Um, K.E. O'Connor, J.I. Jiménez, Genome analysis of the metabolically versatile Pseudomonas umsongensis GO16: the genetic basis for PET monomer upcycling into polyhydroxyalkanoates, Microb. Biotechnol. 14 (2021) 2463–2480, https://doi.org/10.1111/1751-7915.13712.

[45] T. Ishige, A. Tani, Y. Sakai, N. Kato, Wax ester production by bacteria, Curr. Opin. Microbiol. 6 (2003) 244–250, https://doi.org/10.1016/S1369-5274(03)00053-5.

[46] H.M. Alvarez, Triacylglycerol and wax ester-accumulating machinery in prokaryotes, Biochimie 120 (2016) 28–39, https://doi.org/10.1016/J.BIOCHI.2015.08.016.

[47] A. Semai, F. Plewniak, A. Charrié-Duhaut, A. Sayeh, L. Gil, C. Vandecasteele, C. Lopez-Roques, E. Leize-Wagner, F. Bensalah, P.N. Bertin, Characterisation of hydrocarbon degradation, biosurfactant production, and biofilm formation in Serratia sp. Tan611: a new strain isolated from industrially contaminated environment in Algeria, Antonie van Leeuwenhoek, Int. J. Gen. Mol. Microbiol. 114 (2021) 411–424, https://doi.org/10.1007/S10482-021-01527-5/FIGURES/5.

[48] N. Pearcy, M. Garavaglia, T. Millat, J.P. Gilbert, Y. Song, H. Hartman, C. Woods, C. Tomi-Andrino, R.R. Bommareddy, B.K. Cho, D.A. Fell, M. Poolman, J.R. King, K. Winzer, J. Twycross, N.P. Minton, A genome-scale metabolic model of cupriavidus necator H16 integrated with TraDIS and transcriptomic data reveals metabolic insights for biotechnological applications, PLoS Comput. Biol. 18 (2022) e1010106, https://doi.org/10.1371/JOURNAL.PCBI.1010106.

[49] Z. Basharat, F. Tanveer, A. Yasmin, Z.K. Shinwari, T. He, Y. Tong, Genome of Serratia nematodiphila MB307 offers unique insights into its diverse traits, 61 (2018) 469–476. https://doi.org/10.1139/GEN-2017-0250.

[50] X. Song, Y. Ju, L. Chen, W. Zhang, Strategies and tools to construct stable and efficient artificial coculture systems as biosynthetic platforms for biomass conversion, Biotechnology for Biofuels and Bioproducts 17 (2024) 148-, https://doi.org/10.1186/S13068-024-02594-2, 1 17 (2024).

[51] J. Ma, T. Guo, M. Ren, L. Chen, X. Song, W. Zhang, Cross-feeding between cyanobacterium Synechococcus and Escherichia coli in an artificial autotrophic–heterotrophic coculture system revealed by integrated omics analysis, Biotechnology for Biofuels and Bioproducts 15 (2022) 69-, https://doi.org/10.1186/S13068-022-02163-5, 1 15 (2022).

[52] R. Qin, Y. Zhu, M. Ai, X. Jia, Reconstruction and optimization of a Pseudomonas putida-*Escherichia coli* microbial consortium for mcl-PHA production from lignocellulosic biomass, Front. Bioeng. Biotechnol. 10 (2022) 1023325, https://doi.org/10.3389/FBIOE.2022.1023325/BIBTEX.

[53] F. Kratzl, A. Kremling, K. Pflüger-Grau, Streamlining of a synthetic co-culture towards an individually controllable one-pot process for polyhydroxyalkanoate production from light and CO2, Eng. Life Sci. 23 (2023) e2100156, https://doi.org/10.1002/ELSC.202100156;SUBPAGE:STRING:FULL.

[54] G. D'Souza, S. Shitut, D. Preussger, G. Yousif, S. Waschina, C. Kost, Ecology and evolution of metabolic cross-feeding interactions in bacteria, Nat. Prod. Rep. 35 (2018) 455–488, https://doi.org/10.1039/c8np00009c.

[55] D.T. Troiano, M.H.P. Studer, Microbial consortia for the conversion of biomass into fuels and chemicals, Nat. Commun. 16 (2025) 1–12, https://doi.org/10.1038/s41467-025-61957-x, 1 16 (2025).

[56] C. Varrone, I.V. Skiadas, H.N. Gavala, Effect of hydraulic retention time on the modelling and optimization of joint 1,3 PDO and BuA production from 2G glycerol in a chemostat process, Chem. Eng. J. 347 (2018) 525–534, https://doi.org/10.1016/J.CEJ.2018.04.071.

[57] G. Carvalho, I. Pedras, S.M. Karst, C.S.S. Oliveira, A.F. Duque, P.H. Nielsen, M.A. M. Reis, Functional redundancy ensures performance robustness in 3-stage PHA-producing mixed cultures under variable feed operation, N. Biotechnol. 40 (2018) 207–217, https://doi.org/10.1016/J.NBT.2017.08.007.

[58] J.R. Almeida, J.C. Fradinho, G. Carvalho, A. Oehmen, M.A.M. Reis, Dynamics of microbial communities in phototrophic polyhydroxyalkanoate accumulating cultures, Microorganisms 10 (2022) 351, https://doi.org/10.3390/MICROORGANISMS10020351/S1.

[59] J. Sikkema, J.A.M. De Bont, B. Poolman, Mechanisms of membrane toxicity of hydrocarbons, Microbiol. Rev. 59 (1995) 201, https://doi.org/10.1128/MR.59.2.201-222.1995.

[60] L. Yang, X. Pan, R. Zou, Y. Zhang, H. Liu, Environmental and operational stresses in PHA biosynthesis: mechanisms, challenges, and sustainable solutions, Bioresour. Technol. 436 (2025) 133050, https://doi.org/10.1016/J.BIORTECH.2025.133050.

[61] A. Goudarztalejerdi, M. Tabatabaei, M.H. Eskandari, D. Mowla, A. Iraji, Evaluation of bioremediation potential and biopolymer production of pseudomonads isolated from petroleum hydrocarbon-contaminated areas, Int. J. Environ. Sci. Technol. 12 (2015) 2801–2808, https://doi.org/10.1007/S13762-015-0779-0/FIGURES/1.

[62] K. Mahendhran, A. Arthanari, B. Dheenadayalan, M. Ramanathan, Bioconversion of oily bilge waste to polyhydroxybutyrate (PHB) by marine ochrobactrum intermedium, Bioresour. Technol. Rep. 4 (2018) 66–73, https://doi.org/10.1016/J.BITEB.2018.08.013.

[63] M.W. Guzik, S.T. Kenny, G.F. Duane, E. Casey, T. Woods, R.P. Babu, J. Nikodinovic-Runic, M. Murray, K.E. O'Connor, Conversion of post consumer polyethylene to the biodegradable polymer polyhydroxyalkanoate, Appl. Microbiol. Biotechnol. 98 (2014) 4223–4232, https://doi.org/10.1007/s00253-013-5489-2.

[64] T. Ondrovič, E. Hájeková, J. Mikulec, A. Peller, M. Slezáčková, L. Danč, Assessing and improving quality of pyrolysis oil and its fractions from waste polyolefins for refinery use, Ind. Eng. Chem. Res. 64 (2025) 20820–20834, https://doi.org/10.1021/ACS.IECR.5C02341.